國 立 交 通 大 學

機 械 工 程 學 系
碩 士 論 文

Preliminary Study of Gliding Arc Plasma Assisted Catalytic Ethanol

Steam Reforming

利用滑動電弧電漿輔助觸媒將含乙醇水氣重組之初步研究

研究生：徐暐能

指導教授：吳宗信 博士

西元二零一一年七月

利用滑動電弧電漿輔助觸媒將含乙醇水氣重組之初步研究

Preliminary Study of Gliding Arc Plasma Assisted Catalytic Ethanol

Steam Reforming

研 究 生：徐暐能   Student：Wei-Neng Hsu

指導教授：吳宗信 博士   Advisor：Dr. Jong-Shinn Wu

國 立 交 通 大 學
機 械 工 程 學 系
碩 士 論 文

A Thesis
Submitted to Department of Mechanical Engineering
College of Engineering
National Chiao Tung University
in Partial Fulfillment of the Requirements
for the degree of
Master in
Mechanical Engineering

July 2011

Hsinchu, Taiwan

西元二零一一年七月

# 利用滑動電弧電漿輔助觸媒將含乙醇水氣重組之初步研究

學生: 徐暐能　　　　　　　　　　　　　　　指導教授: 吳宗信 博士

國立交通大學機械工程學系

摘要

本實驗係探討利用大氣電漿輔助觸媒經過自熱反應的方式重組原料並進行產生氫氣之研究。利用脈衝電漿產生滑動電弧電漿，電漿氣體為空氣、水和乙醇的混合，並操作在一大氣壓的條件下產生電漿。期望以電漿氣體高能量的特性，幫助前處理重組燃料，以提高利用觸媒產生氫氣的效率。本實驗首先分開探討觸媒產氫與滑動電弧產氫。在觸媒產氫的實驗之中，透過交通大學應用化學研究所李積琛老師及其學生協助觸媒(5 wt% Rh/CeO_2)的製備，並著手探討實驗參數對效率之影響。藉由調整實驗參數達到效果最佳化，其中在低空氣流量 1.0 SLM、0.7 碳氧原子比、反應氣體溫度 160 ℃之條件下，最佳化的氫氣選擇比 115.03%，一氧化碳選擇比 66.02%，轉換率 100%而效率為 63%，另外，在滑動電弧電漿產氫研究中，藉由調整空氣流量、碳氧原子比和輸入功率，來達到產氫效率最佳化。滑動電弧產氫的最佳效率及其參數如下：在較高空氣流量 1.5 SLM、0.7 碳氧原子比、反應氣體溫度 160 ℃和 223 瓦功率輸入之下可達到氫氣選擇比 42.50%，一氧化碳選擇比 68.79%，轉換率 39%而效率為 8%。

最後結合電漿輔助觸媒(5 wt% Rh/CeO_2)產氫，在高流量下電漿可確實提升產氫效

果(在空氣流量 1.5 SLM、0.7 碳氧原子比、反應氣體溫度 160 ℃之條件下，之下，觸

媒產氫的效果降低許多: 氫氣選擇比 78.65%，一氧化碳選擇比 61.27%，轉換率 97%

而效率為 48%)，電漿輔助觸媒在 1.5 SLM 空氣流量、0.7 碳氧原子比、反應氣體溫度

160 ℃、223 瓦的功率輸出之下可達到 111.20%氫氣選擇比、65.52%一氧化碳選擇比、

100%轉換率，效率為 58%。由以上實驗研究可知，大氣滑動電弧電漿輔助觸媒產氫相

當有潛力。
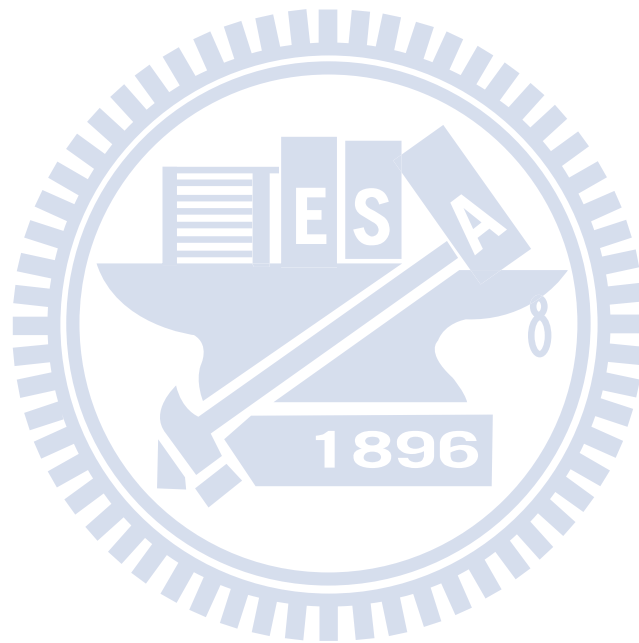
Preliminary Study of Gliding Arc Plasma Assisted Catalytic Ethanol Steam Reforming

Student：Wei-Neng Hsu   Advisor：Dr. Jong-Shinn Wu

Department of Mechanical Engineering

National Chiao Tung University

Abstract

In this study, the gliding arc non-thermal plasma would assist catalyst reforming ethanol into hydrogen through auto-thermal reaction. The plasma discharge gas containing high energy state ions and metastable species which may break the fuel into smaller gas molecular to assist catalyst reforming. At first, catalyst reforming and gliding arc plasma have been separately studied. On one hand, 5 wt% Rh/CeO_2 catalyst reforming has optimized 115.03 % hydrogen selectivity, 66.02 % carbon monoxide selectivity, 100 % conversion rate and 63 % efficiency under 1.0 SLM air flow rate, C/O ratio 0.7 and gas temperature 160 ℃. On the other hand, the optimized plasma-alone reforming results were 42.50 % hydrogen selectivity, 68.79 % carbon monoxide selectivity, 39 % conversion rate and 8 % reforming efficiency under 1.5 SLM air flow rate, C/O ratio 0.7, gas temperature 160 ℃ and plasma absorption power 223 W.

Finally, the PAC reforming experiments were conducted at 1.5 SLM air flow rate (Under 1.5 SLM air flow rate, C/O ratio 0.7 and gas temperature 160 ℃, the catalyst reforming was 78.65 % hydrogen selectivity, 61.27 % carbon monoxide selectivity, 97 % conversion rate and 48 % efficiency), C/O 0.7, plasma absorption power 223 W and gas temperature 160 ℃ and reforming results were 111.20 % hydrogen selectivity, 65.52 % carbon monoxide selectivity, 100 % conversion rate and 58 % efficiency. In summary, the gliding arc plasma assisted catalyst (5 wt% Rh/CeO$_2$) reforming is regarding as a promising technology.
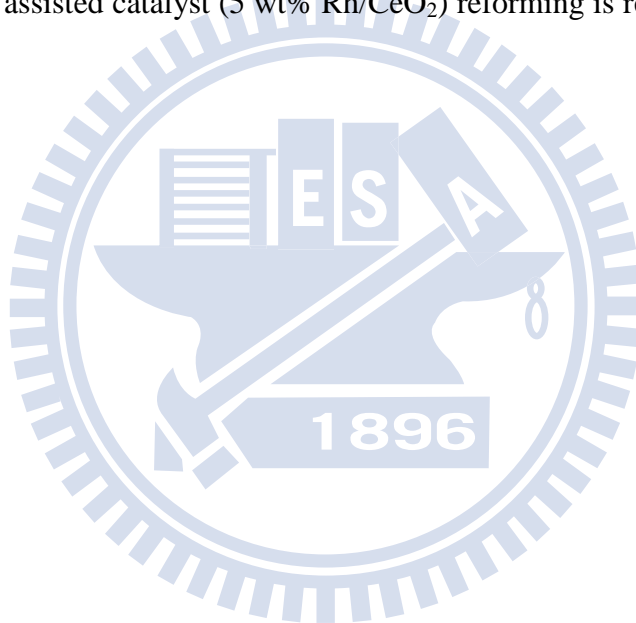
誌謝

在交通大學學習的這兩年過程中，有很多人提供幫忙，不管是實驗上還是生活上。特別感謝指導教授吳宗信教授，有吳教授的指導在這兩年所遭遇到的困難都有所解決。另外也感謝交通大學應用化學系的李積琛老師和其學生在化學領域方面的指導，讓我們在跨領域的題目中有了幫助。

此外實驗室的學長姐、學弟妹也都有在研究過程中提供協助，非常感謝。有了他們的幫助，才能在歡樂又認真的氣氛中學習、成長。

另外也感謝我大學同學們的同儕，這兩年的生活，大家互相幫助，互相勉勵，一起為研究與生活相互勉勵。

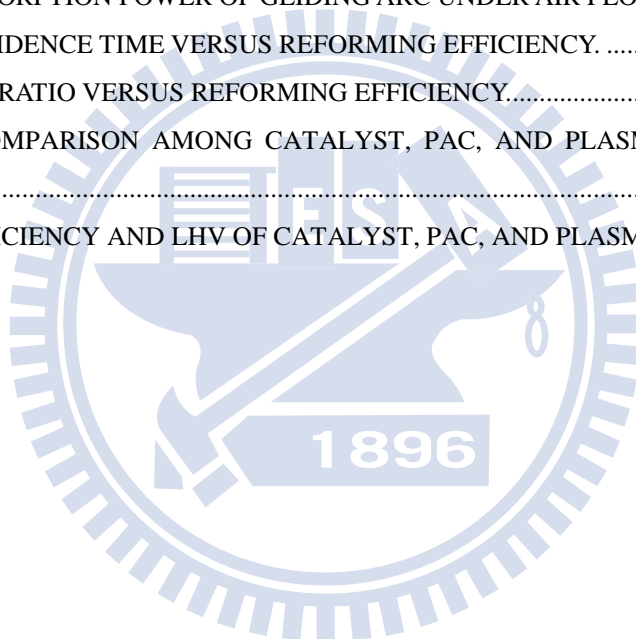最後，感謝家人們的照顧，總是在回家的時候讓我有最溫暖的感覺。

暐能

2011/07/28 于新竹

Table of Contents

List of Tables

List of Figures

Nomenclature

P Input power

V Measuring voltage

I Measuring current

S_{H2} Selectivity of hydrogen

S_{CO2} Selectivity of carbon dioxide

S_{CO} Selectivity of carbon monoxide

S_{H2O} Selectivity of steam
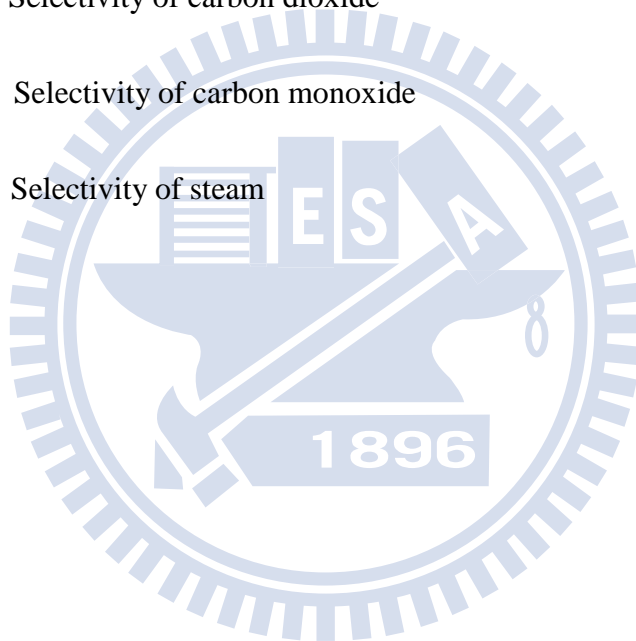
Chapter 1 Introduction

1.1 Background and Motivation

1.1.1 Advantages of Hydrogen Energy

Nowadays, environmental pollutions have become a serious problem due to human activities. Therefore, there is a need to develop alternative clean energy. In many kinds of alternative clean energy, hydrogen energy processes many advantages. Hydrogen gas (H_2) burns cleanly and produces none of any environmental pollutants [Fields S et al., 2003]. Besides, hydrogen gas can be extracted from many sources, including water or fossil fuels (hydrocarbons) such as natural gas or coal. Furthermore, H_2 is definitely a clean energy source and possesses the highest energy content per unit of weight (i.e, 120.7 kJ/g), compared to any of the known fuels. Having these advantages, hydrogen energy has been used for a variety of applications. These applications include providing fuel as the fuel cell used in vehicular propulsion, such as refueling stations for hydrogen powered vehicles. In this context, the hydrogen as a clean fuel appears to be the best future solution for fuel cells and automotive applications [Fouhy K., et al, 1996; Cohn DR., et al, 1997].

High-temperature solid oxide fuel cell (SOFC) has become a potential alternative to hydrocarbon fuel based electricity source, especially for decentralized power system, mainly due to its high thermal efficiency as compared to traditional combustion engines. In addition, carbon monoxide (CO) is a reactive gas in SOFC because of high temperature and

comparably lower bonding energy of CO, while it is considered a very poisonous species for low-temperature proton exchange membrane FC (PEM-FC). Ethanol (heating value of 28.865 kJ/kg) is a green energy which can be produced unlimitedly from corns easily at low cost. Thus, the Center for Green Energy Technology (CGET) of NCTU has started to develop an integrated SOFC system using ethanol as the fuel since 2008 (see Figure 1.1 for the typical test configuration).

1.1.2 Disadvantages of Traditional Reforming Technologies

Hydrogen production from ethanol steam reforming is an endothermic reaction. It requires much heat to maintain the system temperature for thermal equilibrium. Thus, traditional method to produce hydrogen needs power to generate heat and needs space to provide heat generator to process endothermic steam reforming. Moreover, the reaction from ethanol to reform hydrogen needs catalyst to assist reaction pathways perform. Followed are introduction to traditional reforming technologies. There are many reaction pathways which include a number of dehydrogenation and dehydration path [Vizcaino *et al*., 2007] in process, as shown in figure 1.2.

On one hand, the traditional method derived acetaldehyde from dehydrogenation of ethanol such as (2), and then methane and carbon monoxide would be produced through decarbonylation (3). Finally, it produced hydrogen and carbon monoxide from methane steam reforming reaction (4).

$$CH_3CH_2OH \leftrightarrow CH_3CHO + H_2 \tag{2}$$

$$CH_3CHO \leftrightarrow CH_4 + CO \tag{3}$$

$$CH_4 + H_2O \leftrightarrow CO + 3H_2 \tag{4}$$
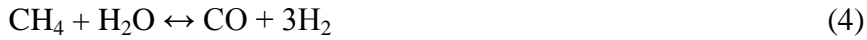
On the other hand, ethylene would be produced from ethanol dehydration reaction (5), followed by dehydrogenation reaction (6) which produce carbon accumulation that deactivate the catalyst. As mentioned above, ethanol steam reforming should avoid it [Vizcaino *et al*., 2007].

$$CH_3CH_2OH \leftrightarrow C_2H_4 + H2O \tag{5}$$

$$C_2H_4 \leftrightarrow 2C + 2H_2 \tag{6}$$

$$C_2H_4 + H_2O \leftrightarrow CO + 4H_2 \tag{7}$$

$$CO + H_2O \leftrightarrow CO_2 + H_2 \tag{8}$$
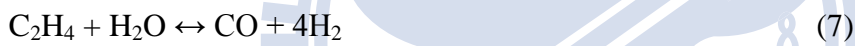
In order to increase the yield of hydrogen, water gas shift, (8), reaction should also involve in total reaction. Thus, the catalyst plays an important role in ethanol steam reforming. The catalyst can be divided into nobel metal and non-nobel metal described as followed:

1. Nobel metal catalyst

The advantage of noel metal catalyst is highly active, such as Ruthenium (Ru), Rhodium (Rh), Palladium (Pd) and Platinum (Pt). Table 1.1 shows properties of ethanol steam reforming with different nobel metal catalysts.

2. Non-nobel metal catalyst

Some non-nobel metals can also be used as hydrogen reforming catalyst which include

nickel (Ni), copper (Cu), zinc (Zn) and cobalt (Co). Table 1.2 shows detailed performances of

ethanol steam reforming using different non-nobel metal catalysts. In table 1.2, the results of

nickel assist reforming is the most effective catalyst among the others; the ethanol in the

reforming process break the carbon bond and produce hydrogen easily. Furthermore, nickel is

not only the most effective catalyst but also the easiest and cheapest element to prepare among

the others, which is the most common catalyst for ethanol steam reforming.

Ethanol fuel is first steamed and then flows through a catalytic reformer, which is made of

rare earth metal oxide consisting of Ce. Although tests at the CGET of NCTU and previous

studies in the literature showed very promising hydrogen conversion efficiency (>100%,

excluding the hydrogen coming from water vapor), it suffers some potential disadvantages,

which include: 1) very high cost of the rare earth material, and 2) short durability of the catalyst.

These two factors may eventually prevent the ethanol SOFC system from real applications in

the future. Thus, how to resolve the above two major shortcomings of the catalytic reformer or

find an alternative reformer is among one of the top priorities of the team. In this thesis, we

found an alternative reformer, plasma assisted catalyst reformer, which is discussed later.

1.1.3 Plasma Assisted Reforming Technologies

Plasma is an ionized gas whose energy state is high, also characterized by a high electrical

conductivity. Application of plasma technologies on hydrocarbon reforming to generate H_2

has been gradually attracted attention due to plasma has following characteristics: fast ignition, the compatibility for a broad range of hydrocarbons, the high energetic density. However, using plasma only to conduct reforming, the H_2 selectivity is generally lower than that achieved with the traditional catalytic reforming process [B. Pietruzk, *et al.*, 2004]. Recently, a new technology has been developed, plasma-assisted catalyst (PAC), which is constructed by integrating plasma and thermal catalysis. The PAC can be applied in hydrocarbon reforming for hydrogen production and gaseous pollutant removal. For the first application, one review paper has been published [M.B. Chang, et al., 2008]. For the latter application, two review papers have also been published [H.H. Ki, et al., 2004; J.V. Durme, et al., 2008].

On the basis of environmental protection, green energy technologies are important. Overall, using PAC to reform hydrogen can combine the advantages of reforming using plasma-alone and using catalyst-alone, in other words PAC reforming has such advantages: rapid startup, fast response time, and fuel flexibility. We expect using PAC could increase the lifetime of the catalyst, reforming performance and H_2 selectivity.

1.1.4 Classification of Plasma Sources

Plasma state is usually classified as the high temperature (or thermal) plasma and the cold (or non-thermal or non-equilibrium) plasma depending on energy level, temperature and electronic density. In the thermal plasma, electrons and other species are thermal

equilibrium thus the temperature can reach to 5000-50,000K, causing the reaction in thermal plasma lacks of chemical reaction selectivity. Those two characters results in very little control over chemical processes inside plasma. Non-thermal plasmas are non-equilibrium in gas temperature and electron temperature, low power requirement and capable to induce physical and chemical reactions within gases at relatively low temperatures. Combining these characters, non-thermal plasma has been applied for fuel gas treatment and has been considered very promising for organic synthesis. A review paper about non-thermal plasma assisted reforming technologies has been published [G. Petipas, et al., 2007]. In the article, it mentioned various kinds of plasma sources as PAC reforming technologies, which are listed in the figure 1.3 and it pointed out the most efficiency plasma sources are gliding arc (GA) and gliding arc in tornado (GAT) by A. Fridman. Plasma generated by the gliding arc discharge which has thermal and non-thermal properties depending on the system parameters such as power input and gas flow rate [A. Fridman, et al., 1999]. Having both thermal and non-thermal properties, gliding arc plasma is possible to obtain the transition regimes of the discharges. In other words, gliding arc plasma can provide non-equilibrium plasma but with higher power levels. These kinds of plasma having both thermal plasma and non-thermal plasma characters are called "intermediate plasma." On the basis of high efficiency hydrogen reforming and the advantages of intermediate plasma, we are proposing using GA as PAC plasma sources.

1.1.5 Comparison between Methane and Ethanol as the Reforming Fuel

Nowadays PAC reforming commonly uses methane as reforming fuel because it can be easily obtained from fossil fuels. However, human-caused global warming is one of the greatest and the most urgent challenges that human need to deal with it on earth today. The main culprit is the enormous amount of the potent greenhouse gas carbon dioxide (CO_2) released into the atmosphere by burning fossil fuels. So far, most of methane was made by fossil fuels (over 80%). In other words, using methane to generate hydrogen as clean fuel could still generate extra carbon dioxide. However, using ethanol instead as methane to generate hydrogen can achieve carbon-nurture. If ethanol can be produced from plants that can consume the greenhouse gasses-CO_2 to produce by photosynthesis in fermentation, the carbon neutral can be achieved. When reforming ethanol into hydrogen, carbon dioxide would be released back to the atmosphere. But the net amount of CO_2 in the atmosphere stays the same [Figure 1.4, L. D. Schmidt, et al., 2004]. Activities that don't disrupt carbon balance in atmosphere are described as carbon-neutral. So, using ethanol as fuel does not raise the level of CO_2 and does not increase global warming.

Hydrogen is difficult to store and transport. Nevertheless, ethanol can solve these problems. Therefore, they can be chosen as the hydrogen carrier for storage and transportation. In comparison of methane and ethanol, the energy storage ability for ethanol is better than methane. Besides, ethanol can exist on the earth in the form of liquid without extra

procedure which is much safer and easier to store and transport than methane. On the basis of the advantages of using ethanol as reforming fuel, we shall emphasize on ethanol reforming.

Nowadays, in the industrial procedure to use ethanol to reform hydrogen is ''steam reforming'' which is widely used all over the world, however the main drawback of this procedure is that it needs an external heat source to support reforming reaction. Furthermore, there was another hydrogen procedure, partial oxidation, had been developed.

In partial oxidation reaction, ethanol reacting with insufficient oxygen generates a slightly endothermic reaction to reform ethanol into hydrogen. However, using this method lowers the performance and brings soot left caused poison of catalyst [A. Fridman *et al*., 2004].

For the sake of solving these problems, combine steam reforming, water gas shift reaction and partial oxidation. Ethanol can be reformed in an ''auto-thermal'' [J.H. Wang *et al*., 2009] process kept both advantages. The chemical reaction showed as followed:

Steam Reforming:

$$C_2H_5OH_{(g)} + H_2O_{(g)} \rightarrow 2CO + 4H_2, \qquad \Delta H_{298} = 254.7 \text{ kJ/mol} \qquad (9)$$

Partial Oxidation:

$$C_2H_5OH_{(g)} + 1/2O_2 \rightarrow 2CO + 3H_2, \qquad \Delta H_{298} = 12.9 \text{ kJ/mol} \qquad (10)$$

Water gas shift (WGS)

$$CO + H_2O_{(g)} \rightarrow CO_2 + H_2, \qquad \Delta H_{298} = -40 \text{ kJ/mol} \qquad (11)$$

Auto-thermal Reforming:

$$C_2H_5OH_{(g)} + 2H_2O_{(g)} + 1/2O_2 \rightarrow 2CO_2 + 5H_2, \quad \Delta H_{298} = -69.4 \text{ kJ/mol} \quad (12)$$
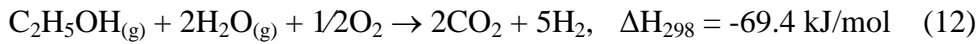
1.1.6 Literature Surveys of Gliding Arc

Since we are interested in developing a PAC system to reform hydrogen, all the following literature surveys are restricted along this line. Table 1.3 summarizes several important features, experiments and parameters in the literature for gliding arc and GAT reforming hydrogen, in which we are interested. Several discussions later are based on the contents of this table.

1.1.6.1 Plasma Power Input Types

Form literature surveys, plasma power input could be divided into AC power supply [Y. Kusano et al., 2008, Z. Bo et al., 2008], DC power supply [A. Fridman et al., 2005], and pulse power supply [H. Shiki et al., 2008]. Table 1.3 summarizes several power input parameters for plasma reactor, and more details are presented in Table 1.4. In the plasma system, gliding arc and GAT, input power could affect plasma characters dramatically, which could also cause synergistic effects on PAC system to change reforming results. However, there has been no systematic work in seriously studying the effects of plasma power to discharge for the same gliding arc and GAT plasma reactor.

1.1.6.2 Geometry and Electrode Design Consideration

For gliding arc plasma reactor, the evolution of gliding arc plasma starts at the shortest

distance (usually 2-5 mm) [A. Fridman et al., 2005, Z. Bo et al., 2007] between two diverging

electrodes when applied voltage reaches the breakdown voltage value. Immediately after

breakdown, the spark channel is formed crossing the gap between the blades. Once the spark

channel is formed, gas flow drags the column downstream and the length of the plasma

column increases. Therefore the diverging electrodes and gas flow rate which lead the column

moving might also change plasma character. There has been a research discussed increasing

electrode gap or decreasing vertical distance between electrode throat and nozzle outlet will

increase higher VOCs decomposition rate [Fig. 1.5, Z. Bo et al., 2007]. However for

hydrogen reforming, discussing how different geometry and electrode design change the

process of reforming is still a critical issue to be resolved.

1.1.6.3 Experimental Measurements

In general, there are two types of measurement regarding plasma system. The first type

is about the electrical properties of the discharge, while the other is about the plasma

diagnostics of the discharge. Typical arrangement of the instrumentation is shown in figure

1.6 [Y. C. Yang *et al.*, 2009] for reference. In the measurement of electrical properties part,

the current and voltage (IV) probe were used to measure time-dependent current and

voltage wave forms. This information can then be used to decide the voltage-current curve,

power-current curve and phase shift between current and voltage. The last one can provide

the information about the magnitude of the resistive component of the discharge.

In the plasma diagnostics parts, it is generally very difficult to measure the discharge properties inside the discharged volume. Thus, most measurements were made in the post-discharge region. They include plasma-parameter measurements using Langmuir-probe technique [Chaudhary *et al.*, 2003] or gas temperature measurements using a thermocouple [Babayan *et al.*, 2001; Wang *et al.*, 2003; Li *et al.*, 2006; Zhu *et al.*,2005], the product gas components were analysis using gas chromatograph [Y. C. Yang et al., 2009; Y. N. Chun et al., 2008; M. B. Chang., et al., 2008], and discharge arc column motion using high speed camera [A. Fridman et al., 2000; Z. Bo et al., 2007]. However in our literature survey, there is no article discussed about OES measurement in hydrogen reforming using gliding arc and GAT. We shall also conduct measuring species concentration (ions and radicals) by using optical emission spectrometry (OES) [M. Kraus et al., 2002; C. Alves et al., 2009].

1.1.6.4 Conversion Rate and Efficiency

From the previous part of survey, the experimental parameters and conditions which could affect PAC system performance have been mentioned. Moreover, in this part of literature survey some parameters that described the performance of reforming hydrogen have been summarized. Conversion rate, efficiency, and selectivity are three important factors to represent the reforming performance. Each of them represents different meanings about reforming product gas composition and formula to calculate the parameter is listed below.

The fuel conversion rate means how much percentage of fuel that were injected into the PAC system have been reformed into other kinds of product; the hydrogen selectivity means how much percentage of hydrogen were formed among all the formed product that contains H atoms. (Similarly, CO selectivity and CO_2 selectivity represent same idea, if there were other formed product gases); the reformer thermal efficiency represents the proportion of the lower heating value (LHV) of formed hydrogen to the input energy, that is the summation of the electrical energy of the plasma and the LHV of the hydrocarbon injected [G. Petitpas *et al.*, 2009].

The methods of data analysis are shown as following Equations.

$$\text{Yield } (H_2) = \frac{\text{Amount of H atoms in the formed } H_2}{\text{Total amount of H atoms injected}}$$

$$\text{Selectivity } (H_2) = \frac{\text{Amount of H atoms in the formed } H_2}{\text{Amount of H atoms in the formed product}}$$

$$\text{Yield} = \text{Conversion rate} \times \text{Selectivity}$$

$$\eta = \frac{(H_2 + CO)_{\text{produced}} \times \text{LHV } (H_2)}{\text{Input plasma energy} + \text{fuel injected} \times \text{LHV (fuel)}}$$

$$\text{Fuel conversion rate } (\%) = \frac{[\text{Input fuel}] - [\text{Output fuel}]}{[\text{Input fuel}]} \times 100.$$

From literature survey, the conversion rate ranges from 62.6% - 87 % [L. Bromberg *et al.*, 2006; A. Fridman *et al.*, 2002, 2005; Y. N. Chun *et al.*, 2008, 2008; M. B. Chang et al.,

2008; G. Petipas et al., 2007]. The thermal efficiency range from 35% - 75.81% [L. Bromberg

et al., 2006; A. Fridman *et al*., 2002, 2005; Y. N. Chun *et al*., 2008, 2008; M. B. Chang et al.,

2008; G. Petipas et al., 2007].

In our research, we shall find optimum conditions for producing hydrogen from

ethanol in our PAC system, for advanced we shall focus on discussing how other

parameters influence conversion rate, selectivity, and thermal efficiency.

1.2 Specific Objectives of the Thesis

Motivated by the technical advantages and tremendous advantages of PAC reforming

as compared to the traditional reforming, also based on the understanding of the present

development in this field, the objectives of this thesis are summarized as followed:

- The gliding arc reactor was designed based on literature review and its characters

  were diagnosed, including electrical properties and arc column motion.

- The catalyst reforming was studied by adjusting several parameters and the results

  were compared to the literature. By comparing the efficiency with literature,

  making sure that self-designed reforming system is ready to conduct plasma

  assisted catalyst reforming.

- The plasma reforming and catalyst reforming were conducted in different

  experimental conditions. In the end of the thesis, the PAC reforming system were

also preliminary conducted to reforming hydrogen and comparing with previous

results.

Chapter 2 Research Methods and Procedures

2.1 Experimental Facility and Instruments

In this section, the introduction of using PAC system to reform hydrogen is proposed. There are two parts, one is experimental facility including power supply, fuel feeding system, plasma reactor, catalyst preparation, and heating system. The other part is experimental instrument including OES, GC, etc.

2.1.1 Plasma Reactor

In this study, all experiments are conducted at air flow rate ranges from 0.5-2 SLM and to meet for this purpose a small gliding arc reactor was designed. The following figure 2.1 describes the gliding arc reactor dimensions. GA reactor mainly consists of two 30 mm long, 7 mm wide and 2 mm thick knife-shaped electrodes fixed on a Peak bed plate, which can sustain at heat deflection temperature at $315^{\circ}C$ and long term property evaluations at $250^{\circ}C$. For latter on using high-speed camera observation of the arc column motion, a quartz tube with inner diameter 22 mm and 55 mm long is well designed in sealing with Peak bed plate.

2.1.2 AC Power Supply

Gliding arc reactor is supplied with a power supply (PVM500 plasma driver). It has independent voltage control ranges from zero to maximum 20 kV peak-to-peak. And frequency ranges from 20-70 kHz. Though, this power supply is relatively unstable compare to others, its price was low ($449.95). In the next chapter, the influence of different output

power magnitude on electrical character and reforming efficiency was studied in detail.

2.1.3 Fuel Feeding System

In this study, the fuel feeding system controls several experimental parameters: C/O (mole) ratio, air flow rate, and ethanol/water mole ratio. C/O (mole) ratio represents the proportion of input C atoms in the ethanol and O atoms in the air and the ethanol. Ethanol and water mole percentage also is an important parameter that would effects the experiment results dramatically. To control accurate parameters, MFC (Multi-gas MFC,MC-100SCCM-D, Alicat Scientific, 100sccm for max) and gradient pump (930d-1428, Young Lin Instrument, 0.0005 to 1 slm) were used to control the flow rate of dry air pumped from compressor though a dehydration process and ethanol-mixed-water solution. Moreover, high purity (99%) ethanol that contains few impurity and DI water were used as fuel, and they were mixed together using ultrasonic wave producer.

As for the fuel feeding system, a controllable nozzle was connected to a stainless steel tube which inside has special design to step up the gasification effect and also has a thermocouple to measure the fuel temperature. The automatic valve was controlled by an adjustable frequency signal at 12 volt voltage and the duty cycle of the frequency was set at a constant cycle: 10/500 to control the valve on and off.

2.1.4 Heating System

In the ethanol steaming reforming, the reactant consisted of water and ethanol needs to

be heated in everywhere along the reaction pipeline, started at fuel injection tube to GC analysis ended. Especially, there are two parts of pipeline need to be heated for specific temperature control, gasification and catalyst reaction. The heating system consisted of two heating furnace, each of it is 30 cm long and can control temperature through a thermal controller. The gasification furnace supplies the heat to heat up the reactant, and the experiment results indicate the reactant temperature has an optimum setup for reforming efficiency.

2.1.5 Catalyst Preparation

In this study, 5% Rh/CeO2 was used as reforming catalyst, especially thanks to Department of Applied Chemistry, NCTU for sharing the chemicals and skills. In the catalyst preparation, at first, 1 g porous Al_2O_3 balls used as carrier were pound to small pieces, 1.00-1.41 mm^3, mixed with ethanol solution which dissolved 0.125 g $Ce(NO_3)_3$ and then heated to 50°C to evaporate ethanol. Thereafter, the Al_2O_3 carrier loaded with $Ce(NO_3)_3$ were sintering in 300°C for 5 hours, meanwhile 0.01g $RhCl_3$ ethanol solution was prepared to mix with 10 % $Ce-Al_2O_3$ after sintering. Follow the same procedure to evaporate ethanol, the 10 % $Ce-Al_2O_3$ loaded with 5% $RhCl_3$ were put into the 600°C furnace and access 200 sccm hydrogen gas to proceed reduction reaction within 6 hours to produce 1 g porous Al_2O_3 loaded with 5% Rh/CeO_2.

2.1.6 Experimental Instrumentations

In this section, the experimental facility and instrumentation for the study are listed below in detail.

The experimental instrumentation includes voltage and current probe for electrical measurements, thermocouple for temperature measurements, optical emission spectral for radical concentration measurements and gas chromatograph for gas composition analyses. The most common electrical diagnostic consists of the measurement of the voltage applied to the electrodes and the resultant discharge current. It is also common to use a capacitor connected in series to ground; the voltage across the series capacitor is then proportional to the charge stored on the electrodes. All the above-mentioned parameters were recorded with a Rogowski coil (IPC CM-100-MG, Ion Physics Corporation Inc.) and a high-voltage probe (Tektronix P6015A), respectively, through a digital oscilloscope (Tektronix TDS1012B). The thermocouple (K type) connected to a thermometer will be used to measure the gas temperature distribution in the afterglow region. The optical emission spectral intensity of the GA is measured using a monochromator (PI Acton SP 2500) with a Photomultiplier tube (Hamamatsu R928). It was used to measure the concentration distribution in the post-discharge region to characterize the capability of generating radicals by the system. In addition, hydrogen, carbon monoxide, carbon dioxide and other hydrocarbon were quantified by GC (YL 6100GC with a pulsed discharge helium ionization mode detector (PDHID) and

packed column of Molecular Sieve 5A (80/100 mesh) and Porapak N (50/80 mesh)) by using

the calibration curves separately prepared. The standard gases for calibration were prepared

in bulbs. Moreover, the gas would access through the gas purifier to condense moisture and

remove impurity before analyzing and calibrating.

2.2 Experimental Methods and Test Conditions

Research steps for the PAC reforming are summarized as followed:

2.2.1 Experimental Methods

The self-designed PAC system is show in figure 2.10. The preliminary experimental

methods are separated in two parts, reforming efficiency and gliding arc plasma character

study.

In the reforming efficiency study, ethanol and water were supplied by liquid pump and

dry air from compressor was controlled by MFC. In pre-heat zone, the ethanol and water

were gasified and heated to specific reactant temperature. After that, the reactant flow into

the plasma reactor. And following is the catalyst reactor where 5 wt% Rh/CeO_2 catalyst was

kept processing reforming reaction. The catalyst reactor temperature was controlled at

constant temperature 380℃. After reforming, the product gas including moisture and

non-converted ethanol were sampled into GC by a 2 m long heating pipeline. Products were

analyzed by gas chromatography, with mass balances closing to within 10 %. As for the

catalyst preparation was mentioned earlier. The preliminary results of hydrogen reforming

were discussed in the next chapter.

In the gliding arc plasma character study, electrodes were connected to power supply system which provides the plasma reactor with bipolar voltage pulses to discharge the gas, air or ethanol-steaming-added air, with different flow rate. Meanwhile, plasma voltage and current were measured and recorded with oscilloscope; arc column motion was recorded with high speed camera. The preliminary results were discussed in the next chapter, also.

2.2.2 Test Conditions

In the catalysis ethanol auto-thermal reforming experiment, air was controlled at 0.5-1.5 SLM; input fuel C/O mole ration was fixed at 0.7; ethanol and DI water proportion was 33.33 mol%; catalyst reactor was maintained at $380^{\circ}C$; Catalyst, 5 wt% Rh/CeO_2, was used. The influence of furnace temperature and air flow rate on selectivity and conversion rate were studied.

In the gliding arc character research, air was controlled at 1.5 SLM. Two kinds of discharge gas were applied, air and ethanol-steaming-added air. C/O ratio was constant at 0.7. The different plasma power were applied to observe the electrical character and the plasma appearance.

In the gliding arc reforming, the influences of air flow rate, C/O ratio and plasma power input to the reforming results were studied. Later on, the optimize conditions of gliding arc were set conduct plasma assisted catalyst reforming.

Chapter 3 Results and Discussion

3.1 Catalyst Reforming

In the catalysis ethanol auto-thermal reforming experiments, the influence of reactant fuel temperature on selectivity and conversion rate has been done. Selectivities of H_2, H_2O, CO and CO_2 are plotted as the function of furnace temperature in figure 3-1. The reforming conditions were fixed at 0.1 SLM, 0.7 C / O ratio, 33.33 % ethanol / water mole ratio and catalyst was 5 wt% Rh / CeO2 (residence time: 12.9 millisecond). The results show none of the minor products are produced and all of ethanol was converted into products, therefore the conversion rate in this experiment was 100%. H_2 selectivity peaks at ~117 % at ~270 ℃ furnace temperature. Due to water gas shift reaction, the added water also converted into H_2 and CO_2; namely, H_2 selectivity exceeded 100% and H_2O selectivity was negative. However, the results show that if furnace temperature was heated over 270 ℃, the H_2 selectivity decreased and the CO_2 selectivity increased. According to the literature survey [L. D. Schmidt et al., 2004], the water gas shift reaction (WGS) would not process in the high temperature, namely, water would not reform into hydrogen causing hydrogen selectivity decreased. Moreover, in the lack of WGS reaction, the heat that used to release from WGS reaction would not provide into total reaction causing the steam reforming which is a strong endothermic reaction would not process. In theory, the CO_2 content would increase and H_2O selectivity would increase, which matched the experiment results.

21

Figure 3.2 showed that the reforming efficiency over different air flow rate at C/O ratio

0.7. At 1.0 SLM air flow rate, the S_{H2} were over 100 %, and the conversion rate was 98 %.

However, when the flow rate increased to 1.5 SLM, the reforming efficiency was poor

compared with low flow rate. Conversion rate and S_{H2} both decreased dramatically. Later on,

the PAC reforming experiments were focused at 1.5 SLM air flow rate, hoping that the

plasma assisted catalyst reforming could improve the reforming results.

3.2 Plasma Reforming

In the section 3.2, the research was focused on gliding arc reforming. First, the visual

observation and electrical character measurement were brought out. Later, the plasma-alone

reforming was studied through adjusting various parameters.

3.2.1 Visual Observation of Gliding Arc

In section 3.2.1, the physical phenomenon of gliding arc were brought out, including

the basic idea of gliding arc, image of gliding arc using air or reforming fuel added air as

working gas and arc column motion recorded by high speed camera.

The gliding arc electrode is composed as a couple of separated electrodes supplied

with a power generator to discharge gas becoming plasma type. The arc starts at the

smallest gap between two electrodes when the electrode field reaches breakdown conditions,

for example, in the atmospheric pressure if the shortest gap between electrodes is 3mm, it

needs 9.6 kV to breakdown the gas, air, forming arc. After the arc starts, the arc current increases very fast, and the voltage of the arc drops. The arc is forced to move to the downstream along electrodes if the gas flow is strong enough. Once the arc moves, it may follow the electrodes' curvature and the arc elongates. In order to sustain the growing arc, the power dissipation increases till the maximum power that can be transferred to the arc from the power supply. When the maximum power is transferred, the arc still continuous growing by the gas flow forced and the energy lost is greater than the power gained. The arc cools down and finally extinguishes. The next cycle starts immediately after the breakdown conditions reached. A typical repetition rate of the arc is in the range from 10 to 100 Hz and changes with the gas flow rate: the higher the flow rate, the higher the frequency [A. Fridman et al., 2002]. There have been some experiments, which the total power and plasma voltage were measured as functions of electrical current and plasma length [A. Fridman et al., 2000]. Figure 3.3 is the experimental electrical circuit. And figure 3.4 showed that when the power of the arc reached maximum value, the arc would not extinguish as fast as it was expected. Instead, the power began to smoothly decrease and plasma channel was still visible for considerable time.

The gliding arc has been called "intermediate" plasma, having both thermal plasma and non-thermal plasma character, which offers greater energy density to perform hydrogen reforming with chemical selectivity.

From the visual observation, the color of the gliding arc changed from white to blue-violet after the ethanol-water solution injected, moreover the area of the discharge were also increased (Figure 3.5 to 3.7). The changed of the working gas changed the composition of the plasma casuing the color and discharge area different. In figure 3.5, the visual observation of the gliding arc are more arc-like and longer comparing to figure 3.6 and figure 3.7 which seems more uniform and flame-like. In the section 3.2.2, the elctrical character under these conditions were mentioned.

In figure 3.8 to 3.10 the arc column motion was captured by high speed camera with 1200 frames per second (Casio, EX-F1) and from (a) to (d) are within a cycle and ordered in time. White dot line in the figure represents a pair of electrodes' location. And the input plasma power parameter was the same in figure 3.8 to 3.10 (The power were set at 50%). In figure 3.8 and figure 3.9, the arc column motion did perform unstable in moving distance. In figure 3.10, two arcs were ignited at the same time. In other words, the new arc ignited before the previous arc exterminated.

3.2.2   Electrical Characterization of Gliding Arc

In the gliding arc electrical characters research, air flow rate was controlled at 1.5 SLM. Three different input power were applied to gliding arc electrode. By integrating plasma voltage and current which were measured by oscilloscope, the plasma absorption power was calculated within different numbers of cycle and showed in the following table 3.1. Table

3.1 showed the plasma absorption power calculated in various numbers of cycles in different input power. From the results, the short period electrical characters of gliding arc were uncertain, in other words the absorption power needs to integrate at least 500 cycles. The table showed that at 30 % of power supply input, the absorption power had maximum values regardless of using air or ethanol steaming added air. Also from the visual observation at 30% of power supply input, the gliding arc plasma was arc-like different from 40 % and 50 % of power supply input which were flame-like. And how the input power affects the hydrogen reforming results were discussed in the following section. In table 3.1 and 3.2, the ethanol steaming added gliding arc plasma had better power absorption efficiency than air-only gliding arc plasma. Comparing to the previous section, visual observation of gliding arc, did find out that ethanol steaming added has longer plasma arc elongations.

Figure 3.11 to 3.13 showed voltage waveform and current waveform versus time under different input power and the voltage pulsed on every 50 μs (20 kHz). In figure 3.11 to 3.13, the peaks of current raised differently in every cycle. The probable reason causing unstable peak current was that the arc column motion may move differently in every cycle. Moreover, same unstable phenomenon was also observed by using high speed camera.

3.2.3 Plasma Reforming Efficiency

In the section 3.2.3, the plasma reforming was studied and the reforming efficiency

was calculated. Through adjusting gas flow rate, carbon to oxygen ratio and input power, the study summarized the optimum parameters setting. The optimum settings for plasma reforming were at 1.5 SLM air flow rate, 0.7C/O ratio and 50% of plasma power input (absorption power: 223 W). And the reforming results were 39 % conversion rate, 43 % hydrogen selectivity and 32 % carbon dioxide selectivity.

3.2.3.1 Effect of Gas Flow Rate

The reactant gas flow rate is one of the parameters that affect the plasma reforming efficiency dramatically. As high as the flow rate, the residence time in the plasma area decrease. Residence time theoretically affects the dissociation and ionization of reactant. Preliminary results of how the gas flow rate and reactant residence time were brought out in section 3.2.3.1 and 3.2.3.3.

In the following figure 3.14 to 3.16, the reforming results were showed. Figure 3.14 represented the conversion rate, hydrogen selectivity and carbon dioxide selectivity versus the gas flow rate at same reactant temperature 160 ℃, 0.7 C/O ratio and the same plasma power 50 % input (absorption power: 223 W). As the flow rate increased from 1.0 SLM to 1.5 SLM, the conversion rate slightly increased, however as the flow rate raised to 2.0 SLM the conversion rate decreased dramatically. And the same trend also appeared on the selectivity of hydrogen. Through the experiment, the 1.5 SLM flow rate condition was viewed as the optimum value, since its conversion rate and hydrogen selectivity were the

highest among other conditions. As flow rate rose up, the conversion rate went down. The probable reason may because the residence time in discharge area was too short to let the reactant reforming well.

In the figure 3.15, the H-selectivity were showed against air flow rate. There was few CH_4 produced barely nothing. The main products that contained H atoms were hydrogen and steaming. The highest hydrogen selectivity was 43 % at 1.5 SLM air flow rate and the H_2O selectivity was about 57 %.

In the figure 3.16, the C-selectivity were showed against air flow rate. There was few CH_4 produced barely nothing. The main products that contained C atoms were carbon dioxide and carbon monoxide. The highest carbon monoxide selectivity was around 75 % at 1.0 SLM air flow rate and the CO_2 selectivity was about 25 %.

3.2.3.2 Effect of Carbon to Oxygen Ratio

C/O ratio is the ratio of C atoms versus the ratio of O atoms in the reforming reactant. (C/O ratio= 2* mole number of ethanol/ (mole number of ethanol+ oxygen)). According to the literature survey [L. D. Schmidt et al., 2004], the C/O ratio is another parameter that affect reforming efficiency dramatically. Figure 3.17 shows that how conversion rate, H_2 selectivity and CO_2 selectivity changed by C/O ratio at 1.5 SLM air flow rate, 160℃ reactant temperature and 50 % of plasma input power (absorption power: 223 W). When C/O ratio was 0.3, the conversion rate was the highest, however the H_2 selectivity was the

27

lowest. When C/O ratio rose to 0.7, the H_2 selectivity was the highest 43 % and conversion

rate was 35 % which was the best reforming results compare to other C/O ratios. This result

also matched the optimum conditions of Rh catalyst reforming [L.D. Schmidt et al., 2004].

Hopefully, the plasma assisted catalyst at C/O ratio 0.7 could have the best efficiency. For

this reason, the preliminary experiments of PAC were conducted at C/O ratio 0.7 and the

results were discussed in the section of 3.3.

In the figure 3.18, the H-selectivity were showed as function of C/O ratio. There was

few CH_4 produced barely nothing. However, when C/O ratio was 0.7, the CH_4 selectivity

was around 3 %. The main products that contained H atoms were hydrogen and steam. The

highest hydrogen selectivity was around 43 % at C/O ratio 0.7 and the H_2O selectivity was

almost 57 %.

In the figure 3.19, the C-selectivity were showed against C/O ratio. There was few CH_4

produced barely nothing. However, when C/O ratio was 0.7, the CH_4 selectivity was around

3 %. The main products that contained C atoms were carbon dioxide and carbon monoxide.

The highest carbon monoxide selectivity was around 85 % at C/O ratio 0.7 and the CO_2

selectivity was about 10 %.

3.2.3.3 Effect of Residence Time

In this section, the effect of residence time that reactant passed through the discharge

were studied. The residence time actually is affected by total flow rate which contains the

air flow rate and the C/O ratio. In fact, it's hard to study whether the residence time or C/O ratio influence the reforming results stronger. Following table 3.3 shows the reforming results in different flow rate which causing different residence time. The table content was based on figure 3.14. According to the table, when the air flow rate rose from 1 SLM to 2 SLM, the residence time decreased from 588 ms to 390 ms. The selectivity of hydrogen were the best at 467 ms (1.5 SLM) and conversion rate were 39%. Dramatically changed of residence time seemed to affect conversion rate stronger.

The table 3.4 were listed to discuss how C/O ratio affects the reforming efficiency. The first two rows were constant at air flow rate 1.5 SLM, and C/O ratio were set at 0.7 and 0.65 (residence time changed from 467.2 ms to 491 ms which were slightly different). The selectivity of hydrogen changed intensively when C/O ratio different from 0.7 to 0.65. By comparing these two tables, the results inferred that the residence time did affect the reforming efficiency, however the C/O ratio affects efficiency stronger.

3.2.3.4 Effect of Input Plasma Power

Figure 3.20 discussed that conversion rate and H_2, CO_2 selectivity as function of the plasma power input. The air flow rate was constant at 1.5 SLM, reactant temperature was 160℃, and C/O ratio was set at 0.7.

In the section of visual observation of gliding arc, the different plasma type were discovered when plasma power input changed from 30 % to 50 %. And the absorption

power was 263 W at plasma power 30 % input, 183 W at plasma power 40 % input and 223

W at plasma power 50 % input. In figure 3.20, when plasma power 50 % input, the S_{H2} was

the highest, 43 %, and conversion rate was 37 %. Interesting, the plasma power 30 % and

40 % input were very different from 50 % plasma power input.

3.3　Plasma Assisted Catalyst (PAC) Reforming

In section 3.3, the preliminary results of plasma assisted catalyst reforming were

discussed. The PAC reforming conditions were set at air flow rate 1.5 SLM, gas temperature

160℃ and C/O ratio 0.7 which is the optimize settings.

3.3.1 Comparison between Plasma, Catalyst and PAC Reforming

In the catalyst reforming experiment, the rose of air flow rate decreased the reforming

efficiency dramatically. In this section, the gliding arc plasma was set up to promote the

catalyst reforming. The experimental conditions were 1.5 SLM air flow rate, C/O ratio 0.7,

and gas temperature 160℃. The results were listed as table 3.5. The PAC reforming had 100

% conversion rate and 111.2 % hydrogen selectivity. Comparing to catalyst reforming and

plasma-alone reforming, the PAC reforming efficiency was improved a lot. The study of

PAC reforming at this stage was rough, in the future, the systematic study of PAC need to

be done.

Table 3.6 showed the efficiency and LHV produced per second in catalyst, PAC and

plasma-alone reforming. Low heating value (LHV) of the product is the low heating value

summation of the carbon monoxide and hydrogen gas. And efficiency means the LHV of product (H_2 plus CO) divided by the LHV of inputted ethanol. The electrical power consumption and the fuel and the catalyst cost were calculated into the total cost. Still, the PAC produced the most of LHV per second and its efficiency reached over 50 %. Though, it needed more cost than catalyst and plasma reforming, PAC reforming still was the most cost-effectiveness.

Chapter 4 Conclusion and Future Work

4.1 Summary

In this study, the plasma reactor, gliding arc plasma, was self-designed. The basic plasma characters, electrical characters and plasma appearance, were diagnosed.

Furthermore, the reforming system which contains plasma reactor, heating reactor, reforming fuel injection system, GC and catalyst preparation was setup well. By comparing the preliminary experiment results with the literature survey, the self-designed catalyst reforming system has been proven well function.

In the catalyst reforming experiment, there was an optimum furnace temperature, 270 ℃, for heating reactant to conduct reforming reaction. And the highest hydrogen selectivity peaks at ~117%.

How the Gliding arc plasma reforming affect by various parameters were studied. The parameters contain air gas glow rate, C/O ratio, residence time, and plasma power input. Under optimized settings, 1.5 SLM air flow rate, C/O ratio 0.7, 160 ℃ reactant temperature and 50% plasma power input, the conversion rate was 31 %, S_{H2} was 42 % and S_{CO2} was 42 %.

Finally, the plasma assisted catalyst reforming was conducted under 1.5 SLM air flow rate, C/O ratio 0.7, 160 ℃ reactant temperature and 50% plasma power input. The conversion rate was 100 % and S_{H2} was 111.2 %. These two indices were higher than

32

plasma and catalyst reforming. The efficiency of PAC reforming was 58%.

4.2 Recommendation of Future Work

The future work of this study are suggested as followed:

1. To compare different mole ratio of ethanol and steam injected.

2. PAC reforming should study in detail and different catalyst should apply to PAC
   system.

3. The optical emission spectral analysis of gliding arc should be done to understand how
   the plasma assists injected fuel reform into hydrogen.

4. To compare different reforming fuel such as methane or propane reforming.

5. We shall develop gliding arc in tornado plasma which promises to have longer
   residence time.
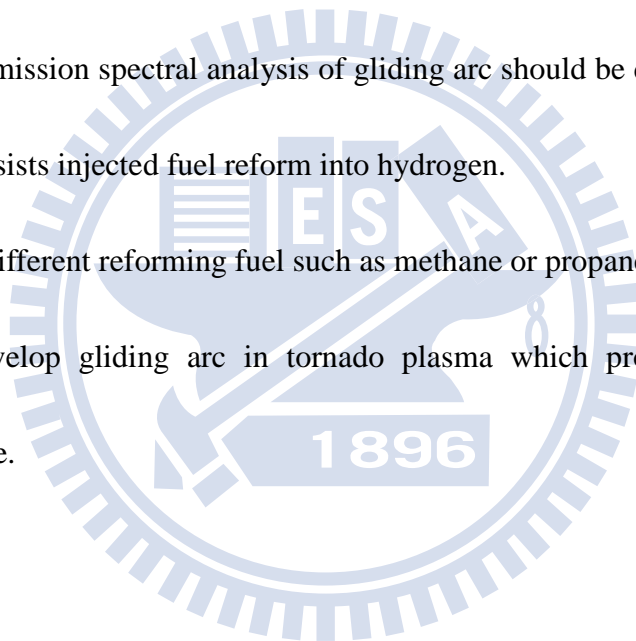
REFERENCES

[1] Batista, M.S., Santos, R.K.S., Assaf, E.M., Assaf, J.M., and Ticianelli, E.A., "High efficiency steam reforming of ethanol by cobalt-based catalysts", Journal of Power Sources, 134, 27-32, 2004.

[2] Bo, Z., Yan, J.H., Li, X.D., Chi, Y., and Cen, K.F., " Scale-up analysis and development of gliding arc discharge facility for volatile organic compounds decomposition", JOURNAL OF HAZARDOUS MATERIALS,Vol.155, No.3, pp.494-501.

[3] Bo, Z., Yan, J.H., Li, X.D., Chi, Y., Cheron, B., and Cen, K.F., "The dependence of gliding are gas discharge characteristics on reactor geometrical configuration", PLASMA CHEMISTRY AND PLASMA PROCESSING, Vol.27, No.6, pp.691-700, 2007.

[4] Bo, Z., Yan, J.H., Li, X.D., et al. "Plasma assisted dry methane reforming using gliding arc gas discharge: Effect of feed gases proportion", INTERNATIONAL JOURNAL OF HYDROGEN ENERGY, Vol.33, No.20, pp.5545-5553, 2008.

[5] Cavallaro, S., Chiodo, V., Freni, S., Mondello, N., and Frusteri, F., "Performance of Rh/Al_2O_3 catalyst in the steam reforming of ethanol: H_2 production for MCFC", Applied Catalysis A: General, 249, 119-128, 2003.

[6] Chao, Y., Huang, C.T., Lee, H.M., and Chang, M.B., " Hydrogen production via partial

oxidation of methane with plasma-assisted catalysis'', INTERNATIONAL JOURNAL

OF HYDROGEN ENERGY, Vol.33, No.2, pp.644-671, 2008.

[7]   Chen, H.L., Lee, H.M., Chen, S.H., et al., '' Review of plasma catalysis on hydrocarbon

reforming for hydrogen production-Interaction, integration, and prospects'', APPLIED

CATALYSIS B-ENVIRONMENTAL,Vol.85, No.1-2, pp.1-9, 2008.

[8]   Cohn, D.R., Rabinovich, A., Titus, C.H., and Bromberg, L., Int. J. Hydrogen Energy, 22,

715–723, 1997.

[9]   Comas, J., Mariño, F., Laborde, M., and Amadeo, N., ''Bio-ethanol steam reforming on

Ni/Al$_2$O$_3$ catalyst'', Chem Eng Journal, 98, 61-68, 2004.

[10] Diagne, C., Idriss, H., and Kiennemann, A., ''Hydrogen production by ethanol

reforming over Rh/CeO$_2$–ZrO$_2$ catalysts, Catalysis Communications'', 3, 565-571,

2002.

[11] Erdohelyi, A., Raskó, J., Kecskés, T., Tóth, M., Dömök, M., and Baán, K., ''Hydrogen

formation in ethanol reforming o n supported noble metal catalysts'', Catalysis Today,

116, 367-376, 2006.

[12] Fatsikostas, A.N., et al., ''Reaction network of steam reforming of ethanol over

Ni-based catalysts'', Journal of Catalysis, 225, pp. 439-452, 2004.

[13] Fields, S., ''Hydrogen for Fuel Cells: Making the Best of Biomass'', *Environ.,* Health

Perspect., 111 (1), A38-A41, 2003.

[14] Fouhy, K., and Ondrey, G., Chem Eng, 103, 46–47, 1996.

[15] Frusteri, F., Freni, S., Chiodo, V., Spadaro, L., Di Blasi, O., Bonura, G., and Cavallaro, S., ''Steam reforming of bio-ethanol on alkali-doped Ni/MgO catalysts: hydrogen production for MC fuel cell'', Applied Catalysis A: General, 270, 1-7, 2004.

[16] Frusteri, F., Freni, S., Spadaro, L., Chiodo, V., Bonura, G., Donato, S., and Cavallaro, S., ''H_2 production for MC fuel cell by steam reforming of ethanol over MgO supported Pd, Rh, Ni and Co catalysts'', Catalysis Communications, 5, 611-615, 2004.

[17] G. Petitpas, J.D. Rollier, A. Darmon, J. Gonzalez-Aguilar, R. Metkemeijer, and L.Fulcheri, ''A comparative study of non-thermal plasma assisted reforming technologies'', International Journal of Hydrogen Energy, Vol. 32, No.14, pp.2848-2867, 2007.

[18] Kalra, C.S., Cho, Y.I., Gutsol, A., Fridman, A., and Rufael, T.S., ''Gliding arc in tornado using a reverse vortex flow'', REVIEW OF SCIENTIFIC INSTRUMENTS, Vol. 99, No.2, 025110, 2005.

[19] Kalra, C.S., Cho, Y.I., Gutsol, A., Fridman, A., and Rufael, T.S., ''Non-Thermal Plasma Catalytic Conversion of Methane to Syn-Gas'', ABSTRACTS OF PAPERS OF THE AMERICAN CHEMICAL SOCIETY, Vol.228, No.1, pp.U687-U687, 2004.

[20] Kalra, C. S., Kossitsyn, M., Iskenderova, K., Chirokov, A., Cho, Y. I., Gutsol, A., and

Fridman, A., Electronic Proceedings of the 16th International Symposium on Plasma Chemistry, Taormina, Italy, pp.22–27, 2003.

[21] Kalra, C.S., Gutsol, A.F., and Fridman, A.A., ''Gliding arc discharges as a source of intermediate plasma for methane partial oxidation'', IEEE TRANSACTIONS ON PLASMA SCIENCE, Vol.33, No.1, pp.32-4, 2005.

[22] Kusano, Y., Teodoru, S., Leipold, F., et al., ''Gliding arc discharge - Application for adhesion improvement of fibre reinforced polyester composites'', SURFACE & COATINGS TECHNOLOGY, Vol.202, No.22-23, pp.5579-5582, 2008.

[23] Kuznetsova I.V., Kalashnikov N.Y., Gutsol A.F., Fridman A.A., and Kennedy L.A. ''Effect of "overshooting" in the transitional regimes of the low-current gliding arc discharge'', JOURNAL OF APPLIED PHYSICS, Vol.92, No.8, pp.4231-4237, 2002.

[24] L. Bromberg, D.R. Cohn, A. Rabinovich, N. Alexeev, A. Samokhin, K. Hadidi, J. Palaia, and N. Margarit-Bel, ''Onboard Plasmatron Hydrogen Production for Improved Vehicles'', PSFC JA-06-3, 2006.

[25] Liguras, D.K., Kondarides, D.I., and Verykios, X.E., ''Production of hydrogen for fuel cells by steam reforming of ethanol over supported noble metal catalysts'', Applied Catalysis B: Environmental, 43, 345-354, 2003.

[26] Llorca, J., Homs, N., Sales, J., Fierro, J.L.G., and Piscina, P.R., ''Effect of sodium addition on the performance of Co–ZnO-based catalysts for hydrogen production from

bioethanol'', Journal of Catalysis, 222, 470-480, 2004.

[27] Llorca, J., Piscina, P.R., Dalmon, J.A., Sales, J., and Homs, N., ''CO-free hydrogen from steam-reforming of bioethanol over ZnO-supported cobalt catalysts: Effect of the metallic precursor'', Applied Catalysis B: Environmental, 43, 355-369, 2003.

[28] Mutaf-Yardimci, O., Saveliev, A.V., Fridman, A.A., and Kennedy, L.A., ''Thermal and non-thermal regimes of gliding arc discharge in air flow'', JOURNAL OF APPLIED PHYSICS, Vol.87, No.4, pp.1632-1641, 2000.

[29] Shiki, H., Motoki, J., Ito, Y., et al. ''Development of split gliding arc for surface treatment of conductive material'', THIN SOLID FILMS, Vol.516, No.11, pp.3684-3689, 2008.

[30] Sun, J., Qiu, X.P., Wu, F., and Zhu, W.T., ''H_2 from steam reforming of ethanol at low temperature over Ni/Y_2O_3, Ni/La_2O_3 and Ni/Al_2O_3 catalysts for fuel-cell application'', Int. J. Hydrogen Energy , 30, 437-445, 2005.

[31] Vizcaino, A.J., Carrero, A., and Calles, J.A., ''Hydrogen production by ethanol steam reforming over Cu–Ni supported catalysts'', Int. J. Hydrogen Energy, 32, 1450-1461, 2007.

[32] Wang, J.H., Lee, C.S., and Lin, M.C., ''Mechanism of Ethanol Reforming: Theoretical Foundations'', JOURNAL OF PHYSICAL CHEMISTRY C, **Vol.**113, No.16, pp**.**

6681-6688, 2009.

[33] Yang Y.C., Lee B.J., and Chun Y.N., ''Characteristics of methane reforming using gliding arc reactor'', ENERGY, Vol.34, No. 2, pp. 172-177, 2009.

[34] Yang, Y., Ma, J., and Wu, F., ''Production of hydrogen by steam reforming of ethanol over a Ni/ZnO catalyst'', Int. J. Hydrogen Energy, 31, 877-882, 2006.

Tables

Catalyst (wt%)	Carrier	T (^{o}C)	S/C	Conversion Rate (%)	H$_2$ Selectivity (%)	Reference
Rh (1)	γ-Al$_2$O$_3$	750	3	100	~95	Liguras 2003
Rh (2)				100	~96	
Ru (1)				42	~55	
Ru (5)				100	~96	
Pt (1)				60	~65	
Pd (1)				55	~50	
Rh (5)	γ-Al$_2$O$_3$	650	8.4	100 (started) 43 (100hr)	---	Cavallaro 2003
Rh (3)	MgO	650	8.5	99	91	Frusteri 2004b
Pd (3)				10	70	
Ni (21)				42	97	
Co (21)				55	92	
Ru (1)	CeO$_2$	450	3	56(20min) 25(100min)	35(20min) 24(100min)	Erdohelyi 2006
Rh (1)				80(20min) 57(100min)	83(20min) 72(100min)	
Ir (1)				54(20min) 35(80min)	40(20min) 25(80min)	
Pt (1)				89(20min) 88(100min)	35(20min) 40(100min)	
Pd (1)				33(20min) 25(100min)	32(20min) 18(100min)	
Rh (2)	CeO$_2$	300	8	58.5	59.7	Diagne 2004
		400		100	66.3	
		500		100	69.1	
	ZrO$_2$	300		100	57.4	
		400		100	68.1	
		500		100	71.7	
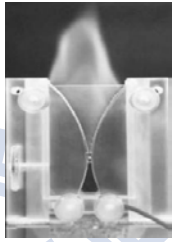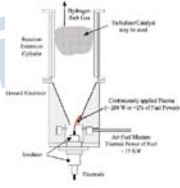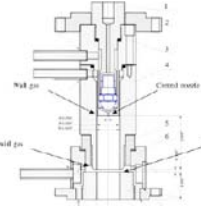
S/C：Mole ratio with water and ethanol
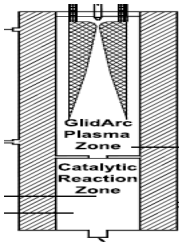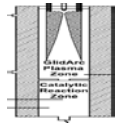
Table 1.1 Properties of ethanol steam reforming with different nobel metal catalysts.

Catalyst (wt%)	Carrier	T (℃)	S/C	Conversion Rate (%)	H$_2$ Selectivity (%)	Reference
Ni (20)	La$_2$O$_3$	773	3	35	70	Fatsikostas 2004
		1073		~100	95	
	γ-Al$_2$O$_3$	973		77	87	
		1073		100	96	
Ni (20.6)	Y$_2$O$_3$	593	3	93	50 (60hr)	Sun 2005
Ni (16.1)	γ-Al$_2$O$_3$			89	44.4(60hr)	
Ni (15.3)	La$_2$O$_3$			100	62.3(60hr)	
Ni (35)	γ-Al$_2$O$_3$	773	6	100	91	Comas 2006
Ni (10)	γ-Al$_2$O$_3$	923	8	100	78.2	Yang 2006
	MgO			100	82.2	
	La$_2$O$_3$			100	89.3	
	ZnO			100	89.1	
Ni (21)	MgO	923	8.5	45(20hr)	95(20hr)	Frusteri 2004
K(1)-Ni(21)				59(20hr)	93(20hr)	
Na(1)-Ni(21)				55(20hr)	95(20hr)	
Li(1)-Ni(21)				83(20hr)	91(20hr)	
Cu(2)-Ni(14)	SiO$_2$	873	3.7	100	71.5	Vizcaíno 2007
Cu(2)-Ni(14)	Al$_2$O$_3$			99.2	50.1	
Co (10)	ZnO	623	13	100(75hr)	73.4	Llorca 2003
Co(10)-Na(0.06)	ZnO	673	13	100	72.1	Llorca 2004b
Co(10)-Na(0.23)				100	73.4	
Co(10)-Na(0.78)				100	74.2	
Co(10)-Na(0.06)		723		100	73.1	
Co(10)-Na(0.23)				100	73.7	
Co(10)-Na(0.78)				100	74.0	
Co (10)	Al$_2$O$_3$	673	3	74	60-70	Batista 2004
Co (10)				99	63-70	
Co (10)	SiO$_2$			89	62-70	
Co (10)				97	69-72	

S/C：Mole ratio with water and ethanol

Table 1.2 Properties of ethanol steam reforming with different non-nobel metal catalysts.

Author	Reactor	Fuel	Reforming process	Flow rate (slm)	Plasma reactor		Performance		
					Electrodes Design	Power (w)	C^1 (%)	S^2 (%)	E^3 (%)
A. Fridman et al. (2005)	Gliding arc	Methane	Pox*	2-10		50	87	N/A	75.81
		Isooctane	ATR** + catalyst			4	75	N/A	48.78
	GAT	Methane	Pox	N/A		200	80	N/A	74
L. Bromberg et al. (MIT 2006)	GEN 2	Methane	ATR + catalyst	30-50		210	103.9	N/A	63.59
	GEN 3	Ethanol	Pox + catalyst	20		200	N/A	N/A	43.5

| Y. N. Chun et al. (2008) | Gliding arc | Propane | Steam*** + CO₂ | 11-20 | | 390-1370 | 62.6 | N/A | N/A |
| | | Methane | Pox + catalyst | 5-30 | (Three gliding arc electrodes connected in 120°) | 1300 | 67 | 93 | 35 |

1. C: conversion rate 2. S: selectivity 3. E: efficiency

Pox*: Partial oxidation reaction. ATR**: Auto thermal reaction.

Steam***: Steam reforming reaction.

Table 1.3 Summary of important features, experiments and parameters for plasma and

PAC reforming.
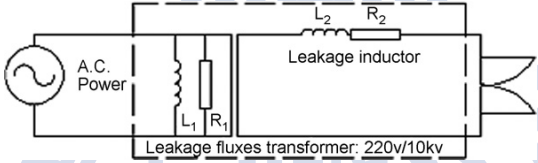
Author	Phase	Power generator	Power input
Y. Kusano et al. (2008)	AC	Power supply (Generator 6030. SOFTAL Electronic GmbH, Germany).	Input power: 1.6-2.2 kW Frequency: 33-40 kHz
B. Zheng et al. (2008)	AC		Input voltage: 10 kV Frequency: 50 Hz
A.Fridman et al. (2005)	DC	Power supply (Universal Voltronics, Inc.)	Input voltage: 10 kV Input current: 0.05-0.15 A
H. Shiki et al. (2008)	Pulse	Pulse modulator (Kurita Seisakusho Co., Ltd., 6 kW) Slide regulator (Matsunaga Seisakusho, S3-2413, 5.2 kVA) High-voltage transformer (Kurita Seisakusho Co., Ltd., 250/12 kV)	Input power: 300 W Pulse frequency: 15-20 kHz Pulse width: 1.6-2.8 μs

Table 1.4 Summary of plasma power input type.

	Instrument	Model	Specifications
1	Rogowski coil (Figure 2.6)	IPC CM-100-MG, Ion Physics Corporation Inc.	Max. peak current: 500A Output sensitivity: 1V/A
2	High-voltage probe (Figure 2.7)	Tektronix P6015A	Max. peak voltage: 40kV Max. Bandwidth:75MHz
3	Thermocouple (Figure 2.8)	K type	Measurement range: -20 °C to +400 °C
4	Gas chromatograph (Figure 2.9)	YL 6100GC	Packed columns: Molecular Sieve 5A (80/100) Porapak N (50/80 mesh)

Table 2.1 Experimental Instruments.

Cycle Absorption Power (W) Power	10	100	300	500	700	1000
30 %	338.56	273.77	274.81	273.77	278.75	263.11
40 %	215.68	191.3	198.38	180.43	182.11	183.3
50 %	146.43	225.6	212.28	225.63	222.05	223.32

Table 3.1 The absorption power of gliding arc under 1.5 SLM air flow rate, C/O ratio: 0.7.

Cycle Absorption Power (W) Power	10	100	300	500	700	1000
30 %	202.88	177.34	177.71	179.68	174.94	170.86
40 %	92.03	124.9	107.53	106.85	107.75	106.47
50 %	103.3	102.48	100.72	100.95	100.98	102.44

Table 3.2 The absorption power of gliding arc under air flow rate 1.5 SLM.

Air Flow Rate (SLM)	Residence time (ms)	C/O	Selectivity (%)		Conversion (%)
			H_2	CO_2	
1	588.16	0.7	38%	27%	37%
1.5	467.21	0.7	42%	32%	39%
2	390.7	0.7	33%	31%	28%

Table 3.3 The residence time versus reforming efficiency.
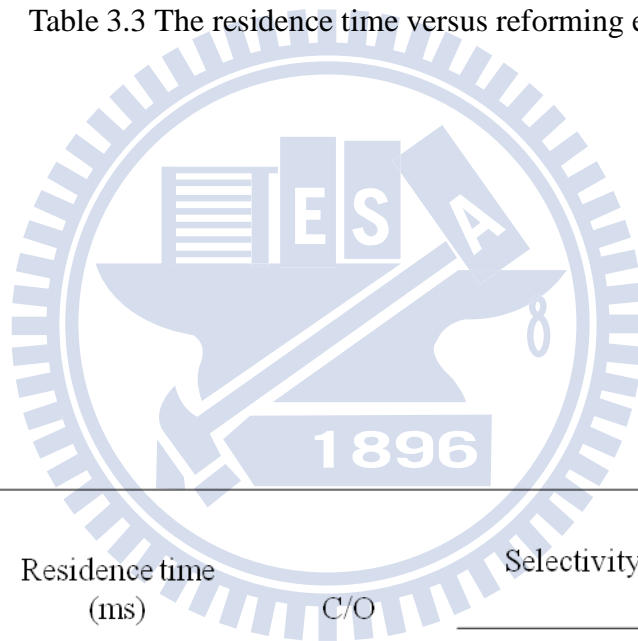
Air Flow Rate (SLM)	Residence time (ms)	C/O	Selectivity (%)		Conversion (%)
			H_2	CO_2	
1.5	467.2	0.7	42%	32%	39%
1.5	491	0.65	24%	33%	32%
2	390.7	0.7	33%	31%	28%
1.5	353	0.8	17%	41%	10%

Table 3.4 The C/O ratio versus reforming efficiency.

Comparison among Catalyst, PAC, and Plasma only Reforming

	Catalyst	PAC	Plasma only
Mass Error	5%	3%	7%
H_2	57.04%	111.20%	42%
CO_2	39.66%	34.48%	32%
CO	60.34%	65.52%	68%
Water	42.96%	-11.20%	58%
Conversion Rate	90.00%	100.00%	39%

Table 3.5 The Comparison among catalyst, PAC, and Plasma-alone reforming efficiency.

	Catalyst	PAC	Plasma only
LHV per second (kJ/s)	5.84	7.26	1.63
Efficiency (%)	40%	58%	8%
Cost (NT)	0.119	0.120	0.071
Cost / LHV	0.020	0.016	0.043

Table 3.6 The efficiency and LHV of catalyst, PAC, and plasma-alone.

Figures
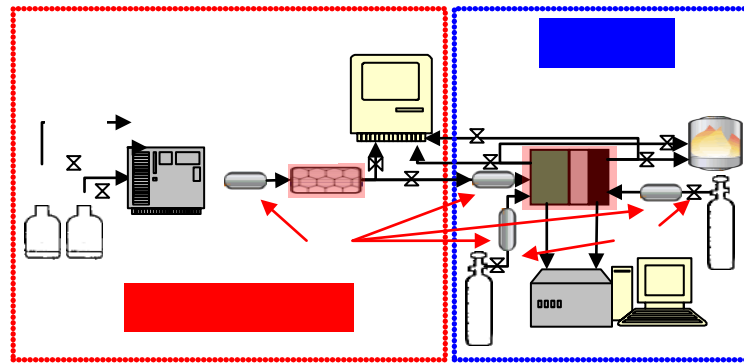
Figure 1.1 Sketch of the typical test arrangement for ethanol reformer (left) and the

SOFC (right) at CGET of NCTU.
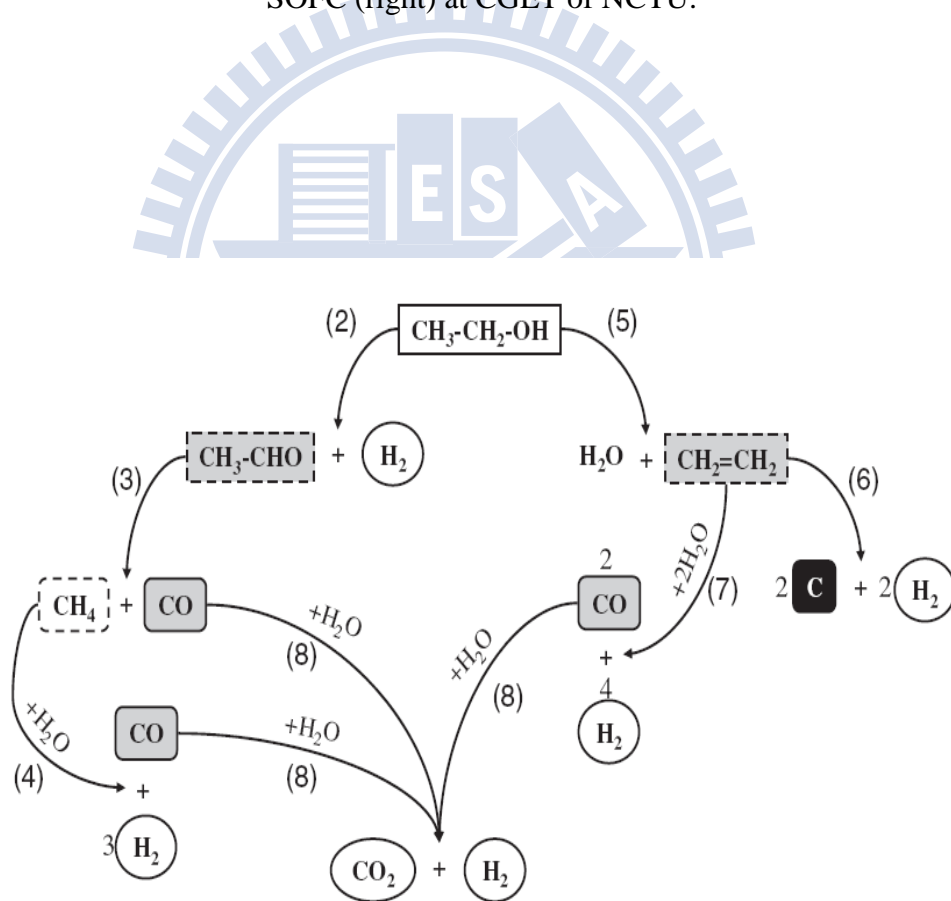
Figure 1.2 The basic reaction of ethanol steam reforming [Vizcaino et al., 2007].
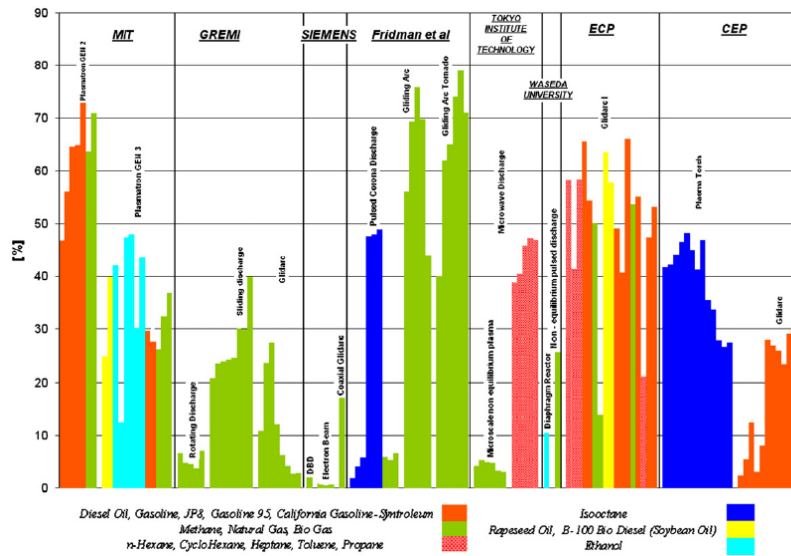
Figure 1.3 The comparison between different plasma reactors [G. Petipas, et al., 2007].
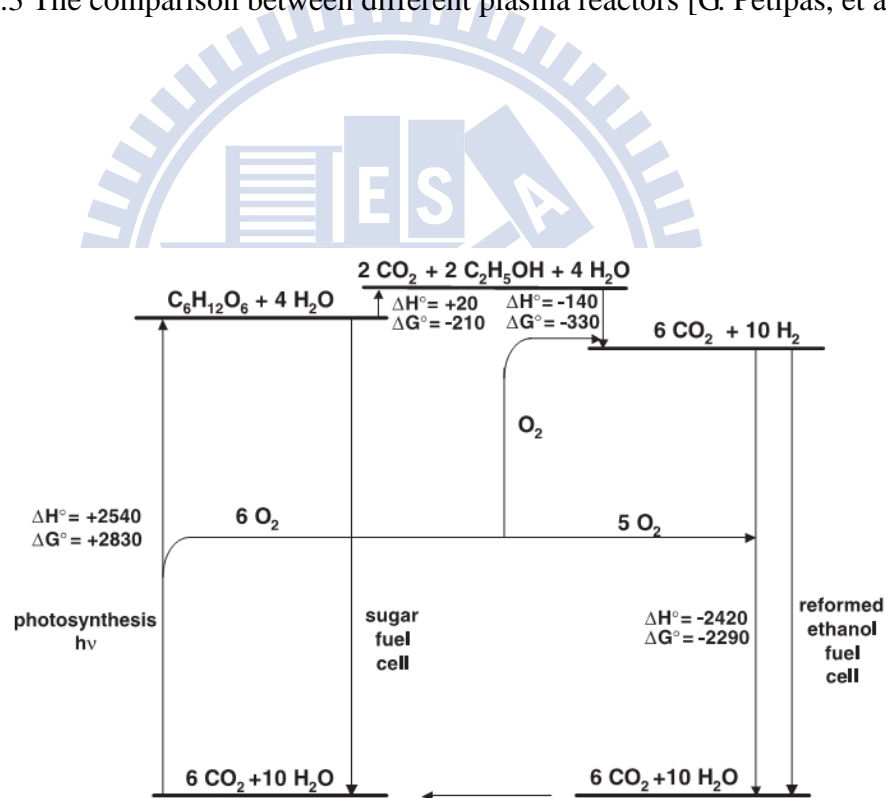
Figure 1.4 An energy diagram indicating the standard enthalpy ($\triangle H°$) and free energy

changes ($\triangle G°$) in kJ/mol for the reactions in a renewable energy cycle operating between CO_2

and biomass [L. D. Schmidt, et al., 2004].
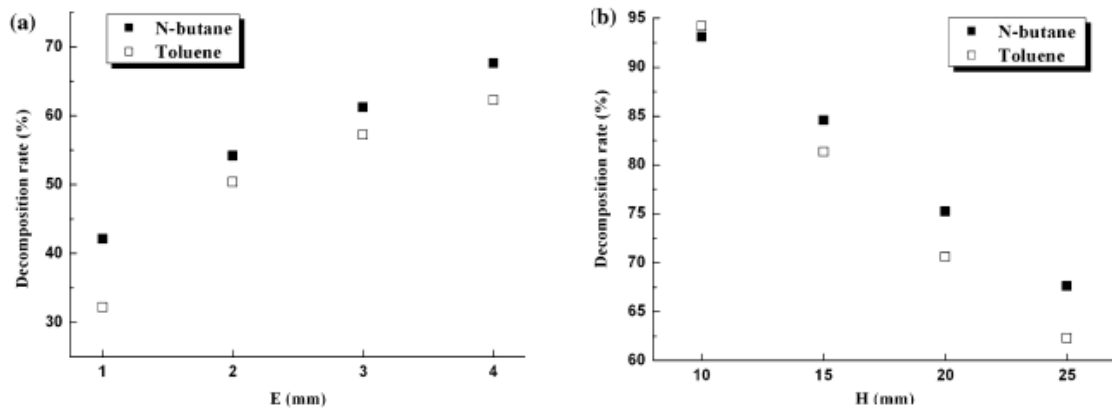
Figure 1.5 Influence of electrode gap (a) and vertical distance between electrode throat

and nozzle oulet (b) on n-butane and toluene decomposition rate [Z. Bo et al., 2007].
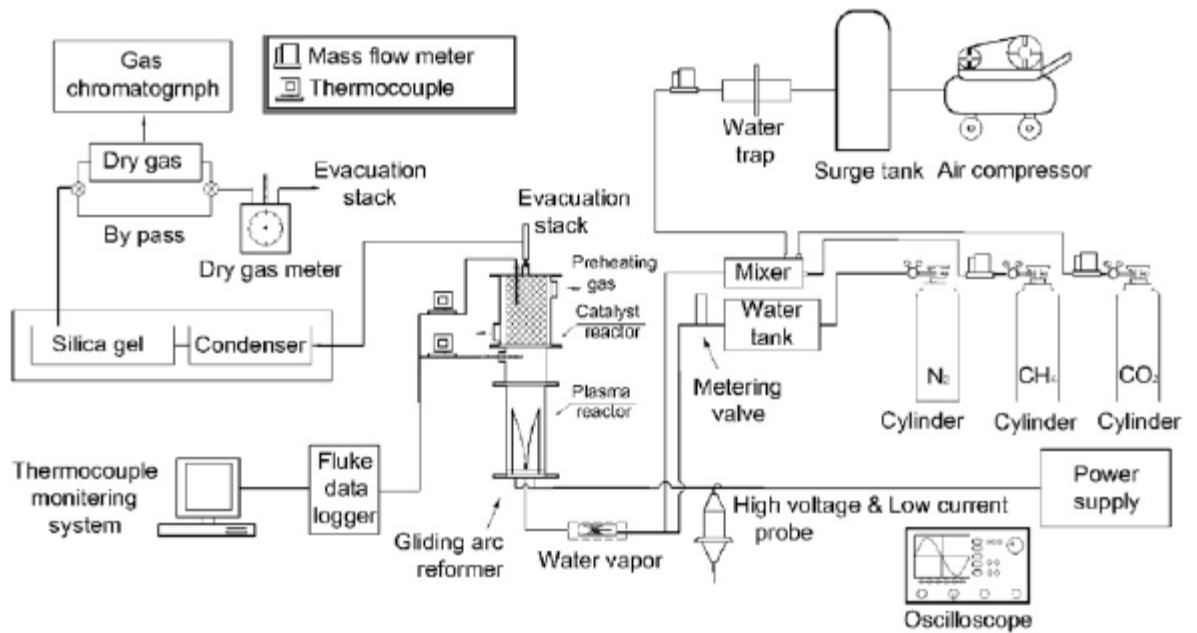
Figure 1.6. Typical arrangement of instrumentation for PAC system [Y. C. Yang *et al.*,

2009].

51
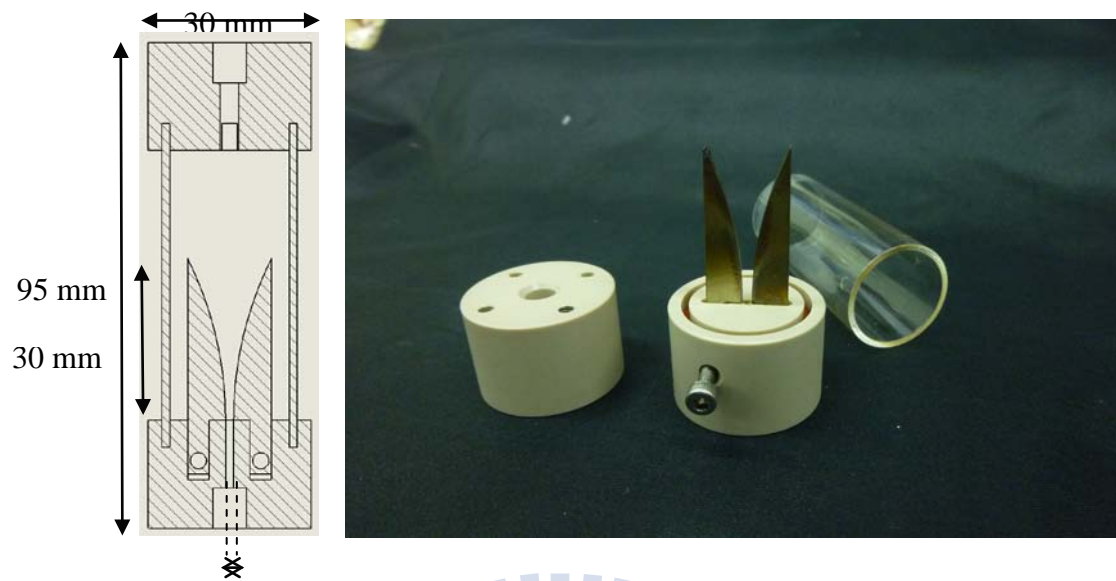
Φ, electrode gap = 1.4 mm

Figure 2.1 The self-designed gliding arc reactor

Figure 2.2 The power supply (PVM500 plasma driver).

Figure 2.3 The fuel feeding nozzle.

Figure 2.4 The MFC and the liquid pump.
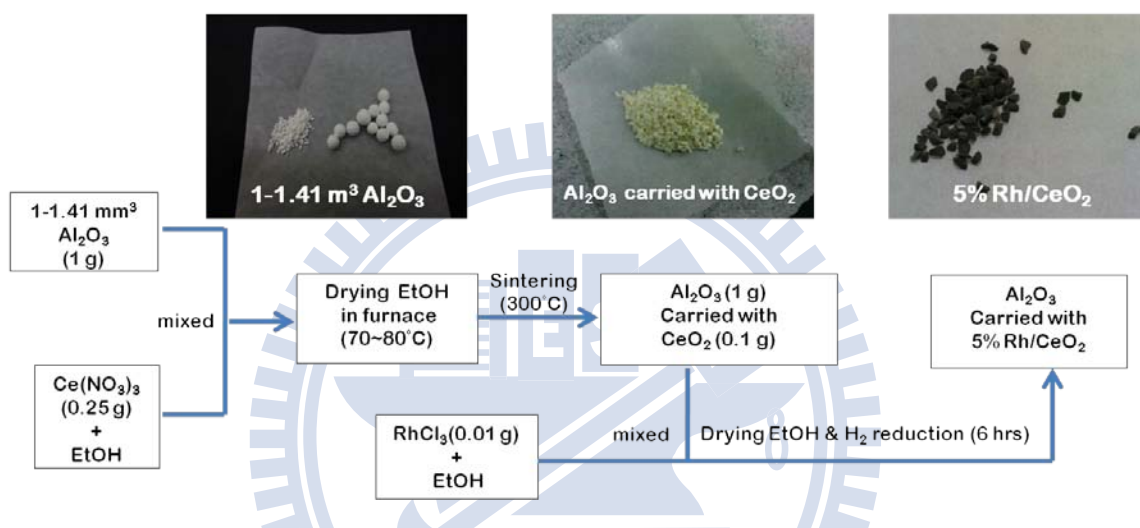
Figure 2.5 The procedure of catalyst preparation.

Figure 2.6 Rogowski coil.

Figure 2.7 High-voltage probe.
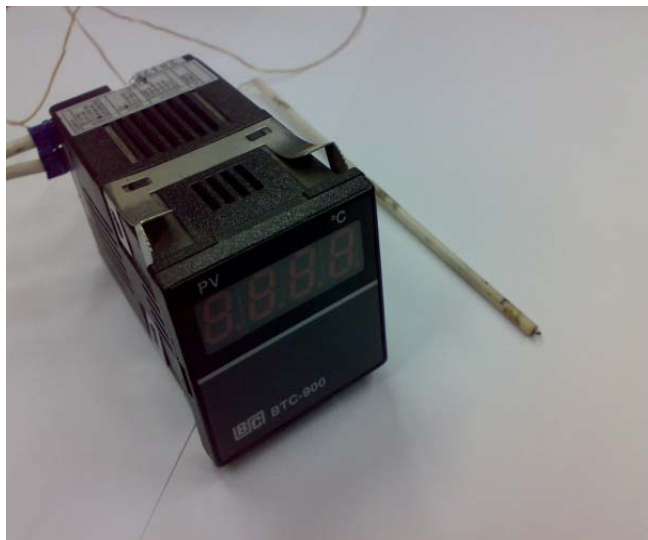
Figure 2.8 Thermocouple.
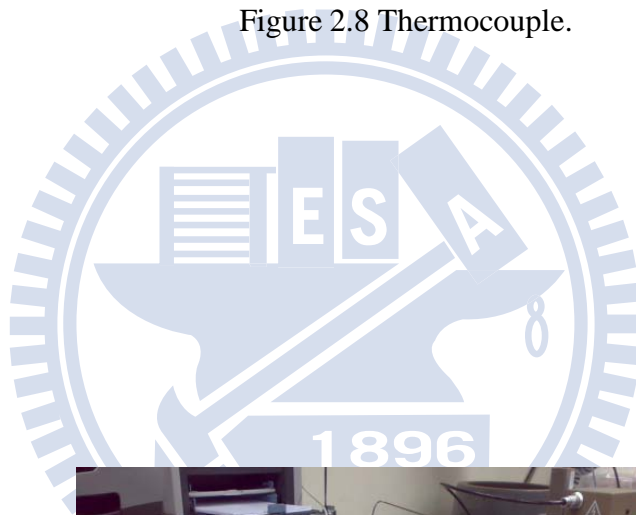
Figure 2.9 Gas Chromatograph.
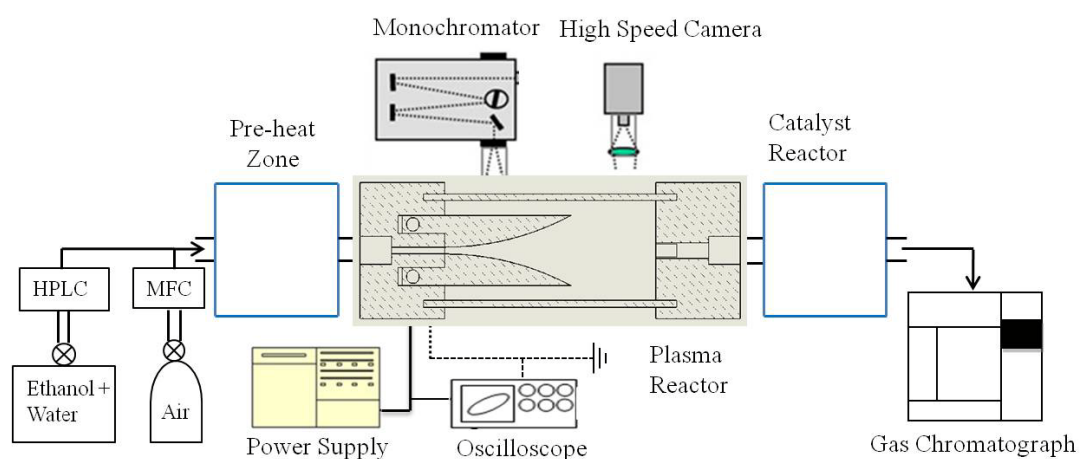
Figure 2.10 The Experimental instrumentation of PAC system.
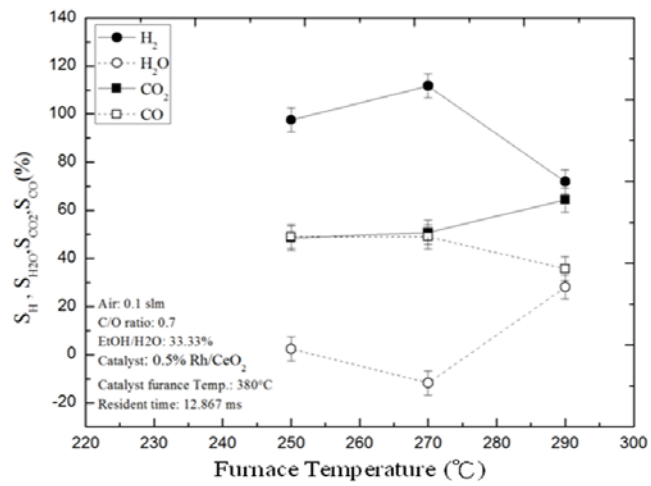
Figure 3.1 The selectivity of hydrogen, water, carbon dioxide and carbon monoxide over

furnace temperature.
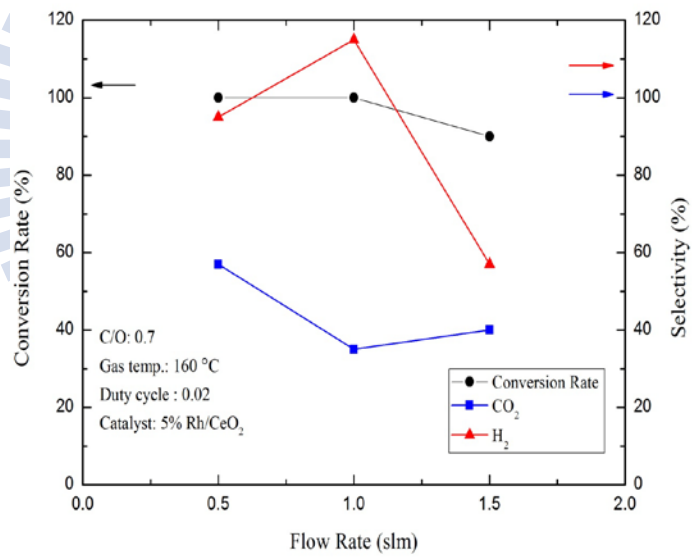
Figure 3.2 The conversion rate, hydrogen and carbon dioxide selectivities over air flow

rate.
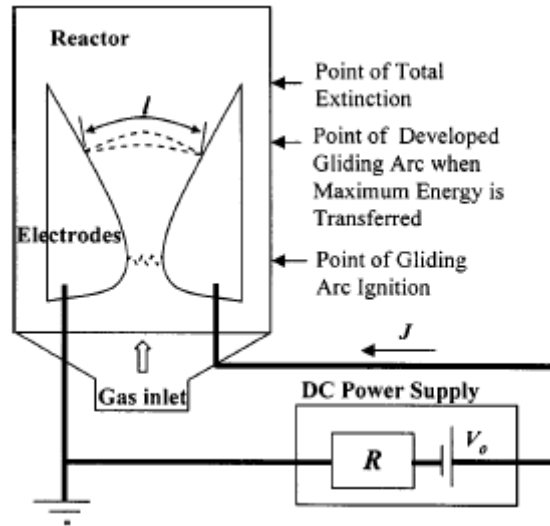
Figure 3.3 Schematic of the electricscheme [A. Fridman et al., 2000].
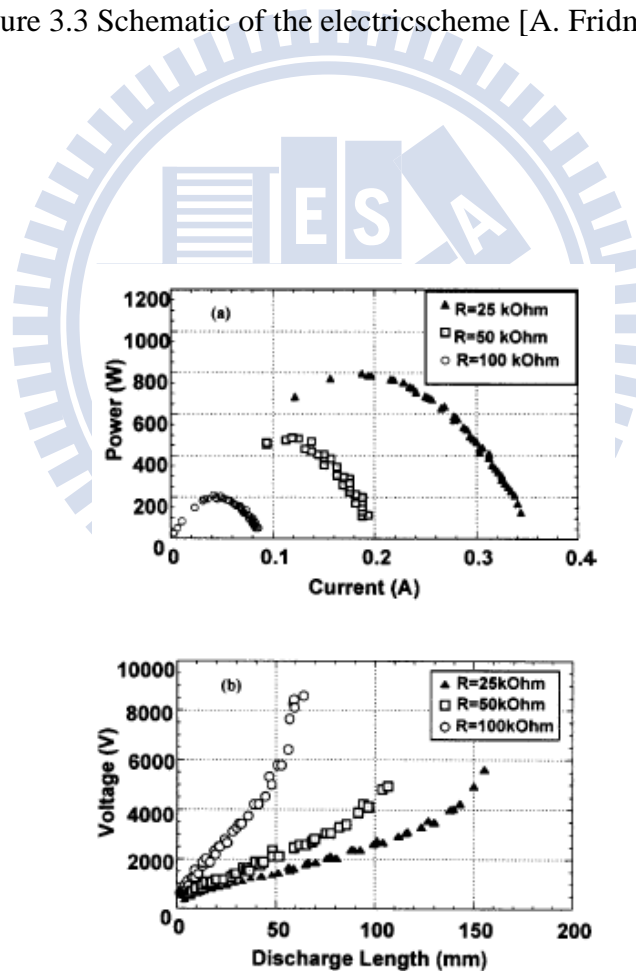
Figure 3.4 (a) Current-total power of the gliding arc; (b) discharge length-voltage of the

gliding arc in (a) [A. Fridman et al., 2000].
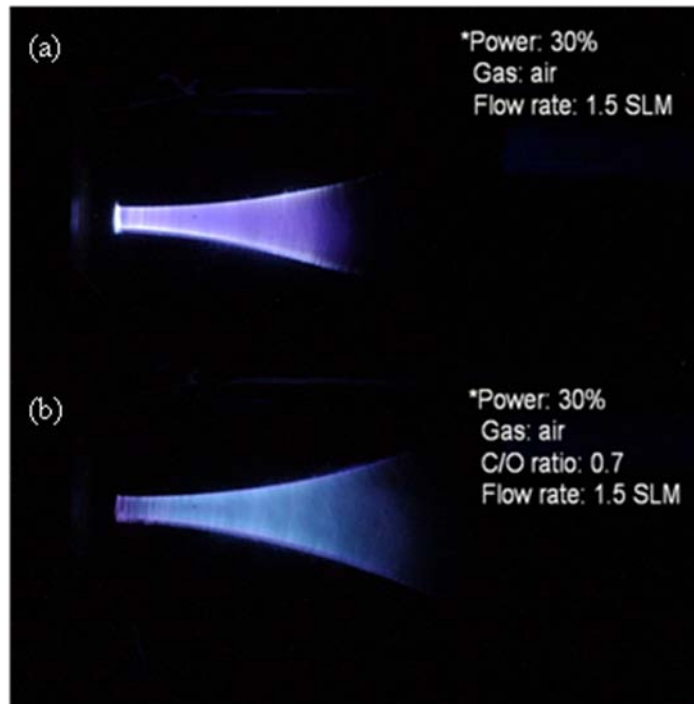
Figure 3.5 Image of gliding arc under power 30%, air flow rate constant at 1.5 SLM and

(a) without and (b) with the ethanol-water solution at C/O ratio 0.7.
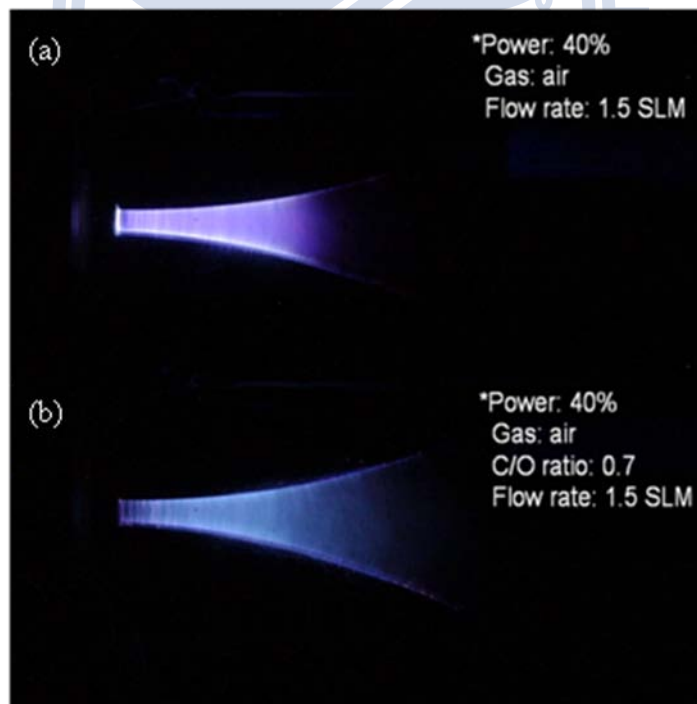
Figure 3.6 Image of gliding arc under power 40 %, air flow rate constant at 1.5 SLM

and (a) without and (b) with the ethanol-water solution at C/O ratio 0.7.
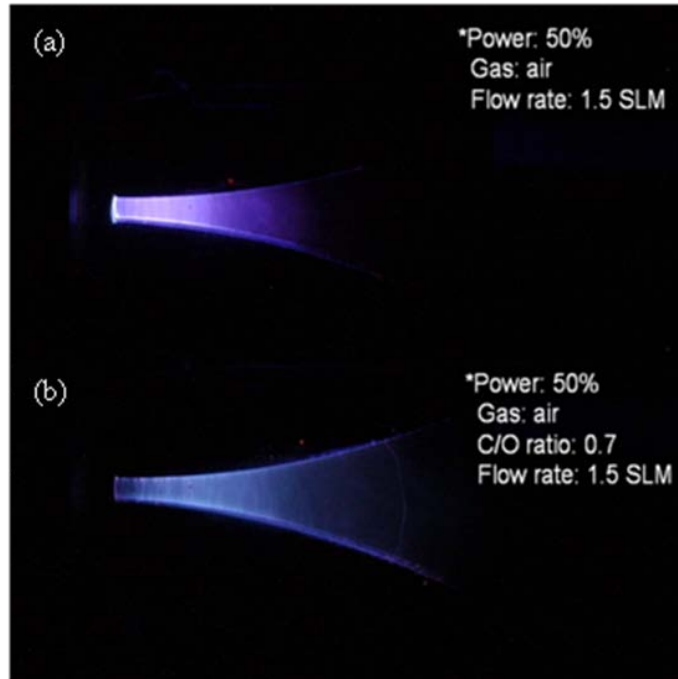
Figure 3.7 Image of gliding arc under power 50 %, air flow rate constant at 1.5 SLM

and (a) without and (b) with the ethanol-water solution at C/O ratio 0.7.
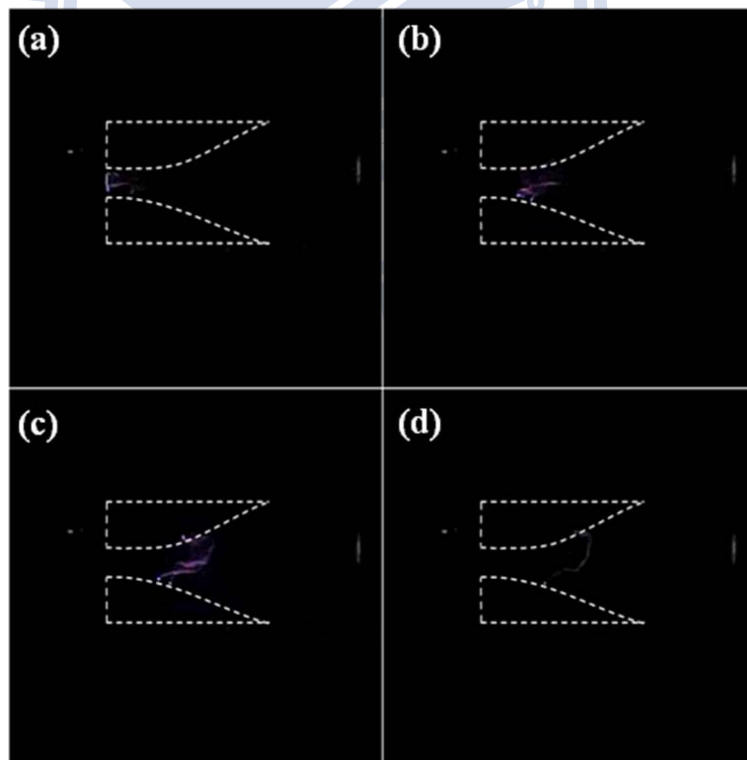
Figure 3.8 The arc column motion when plasma power input 50 %, 1.5 SLM air flow
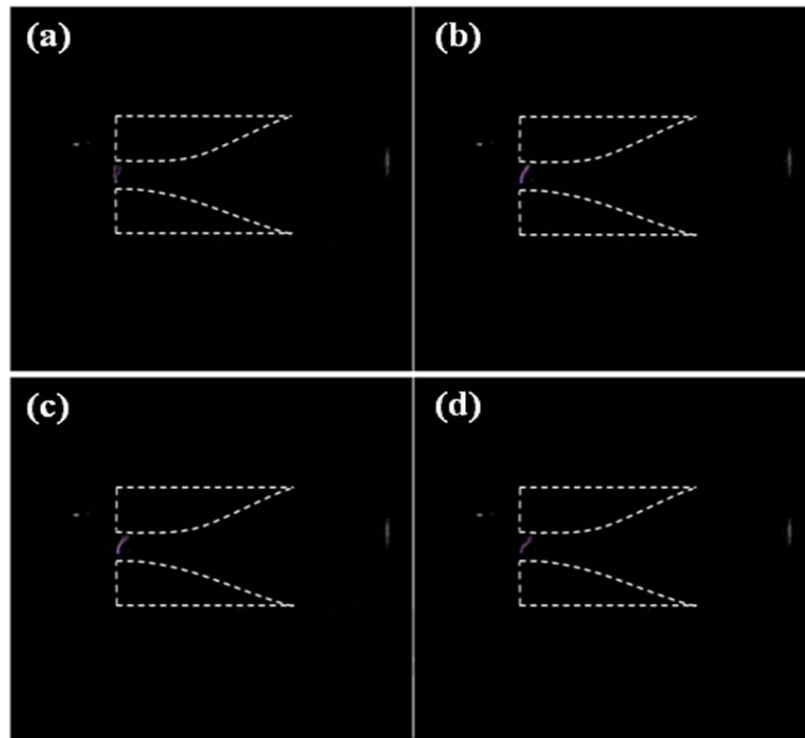
rate. (1200 frames per second)

Figure 3.9 The arc column motion when plasma power input 50 %, 1.5 SLM air flow

rate. (1200 frames per second)
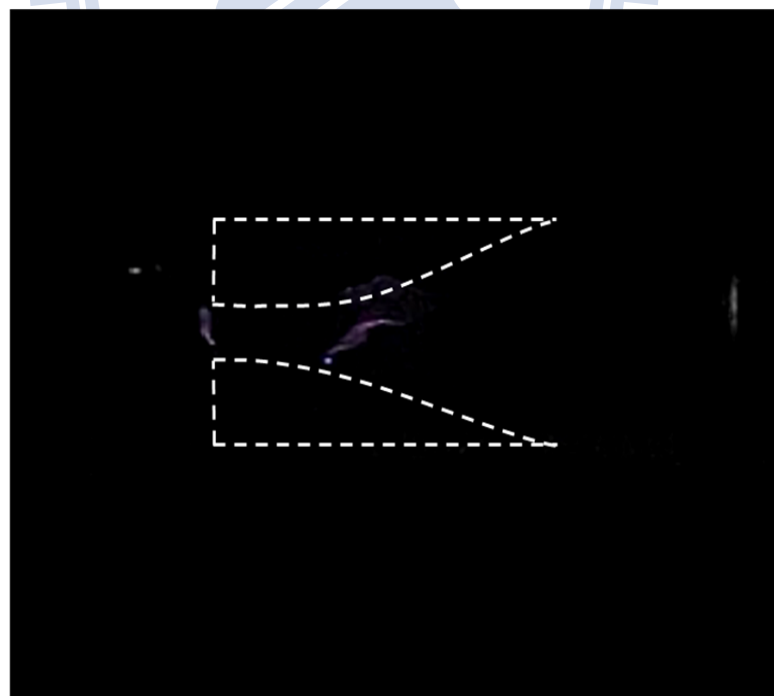
Figure 3.10 The arc column motion when plasma power input 50 %, 1.5 SLM air flow

rate. (1200 frames per second)
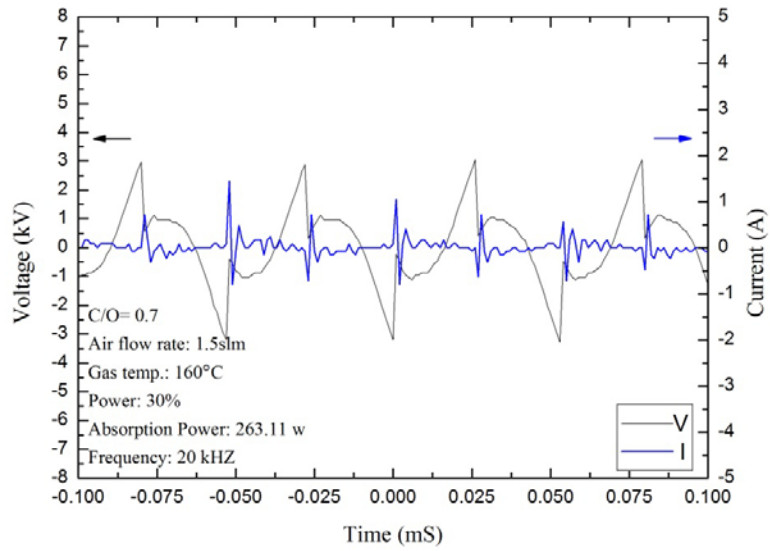
Figure 3.11 Electrical properties for gliding arc when 30% applied power.
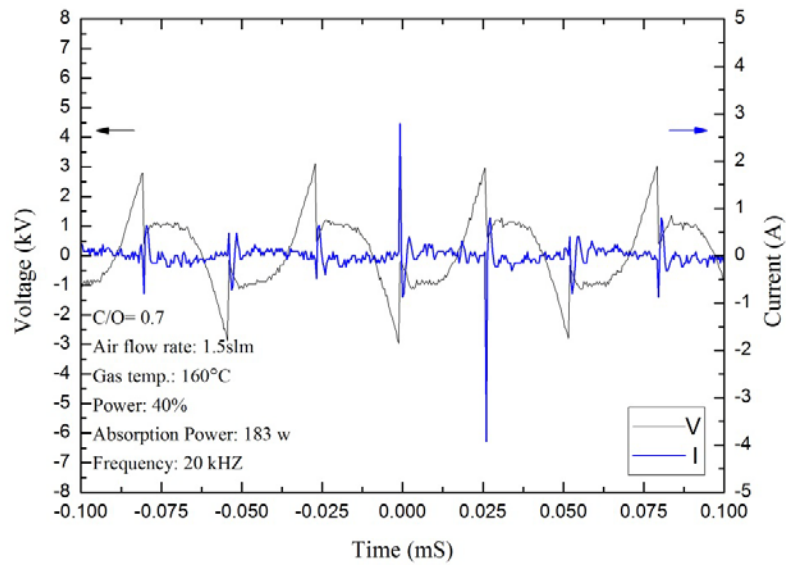
Figure 3.12 Electrical properties for gliding arc when 40% applied power.
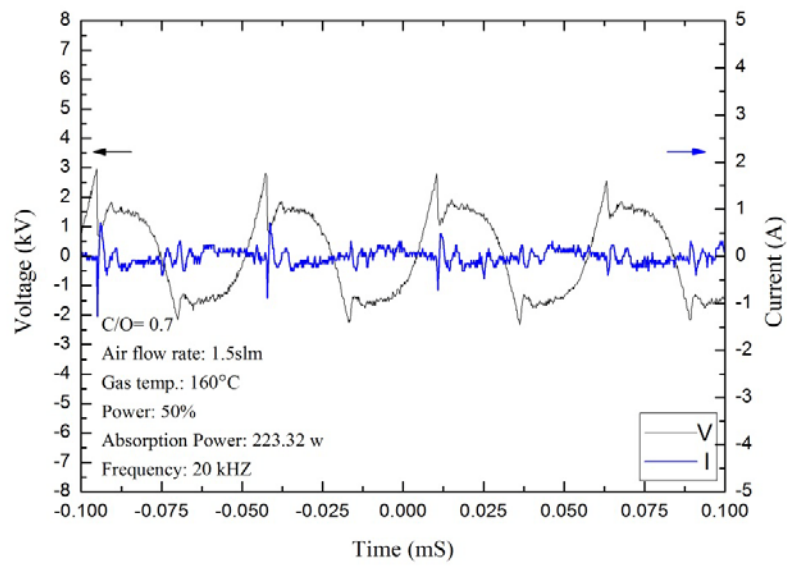
Figure 3.13 Electrical properties for gliding arc when 50% applied power.
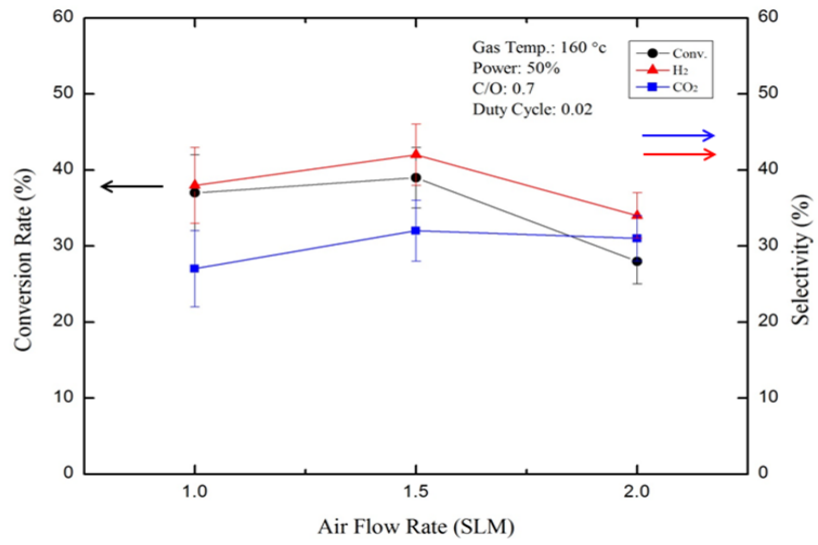
Figure 3.14 Conversion rate, S_{H2} and S_{CO2} versus air flow rate.
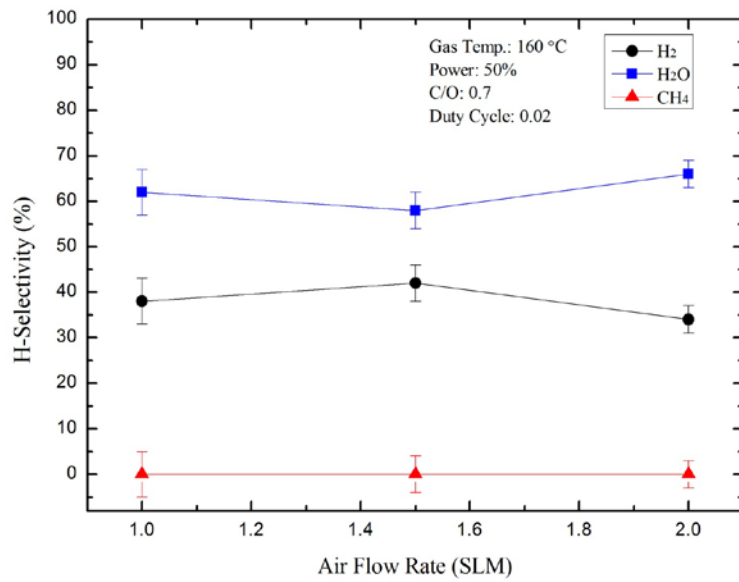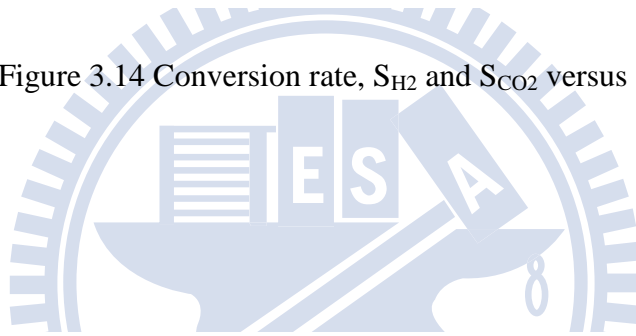
Figure 3.15 S_{H2}, S_{H2O} and S_{CH4} versus air flow rate.
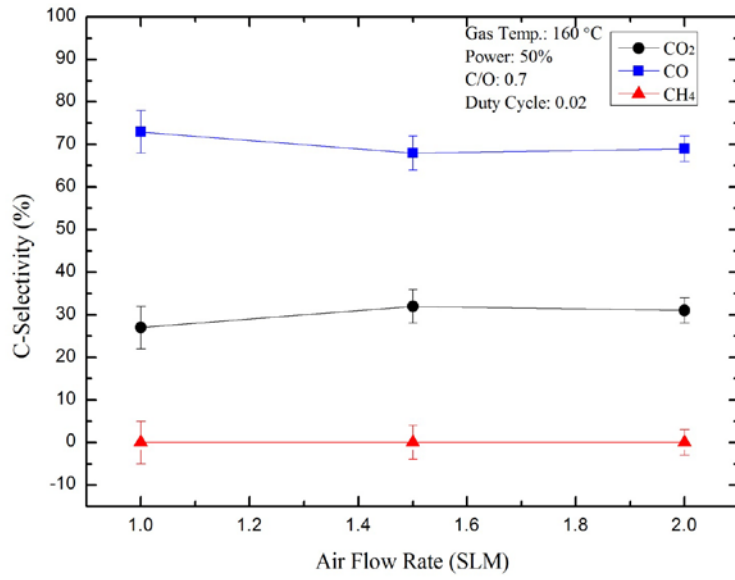
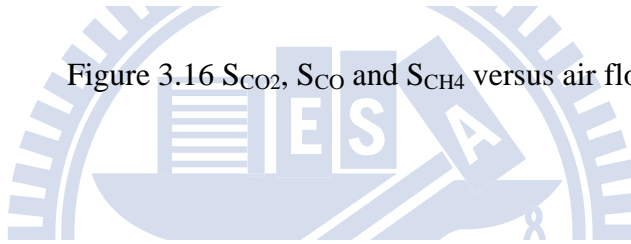Figure 3.16 S_{CO2}, S_{CO} and S_{CH4} versus air flow rate.
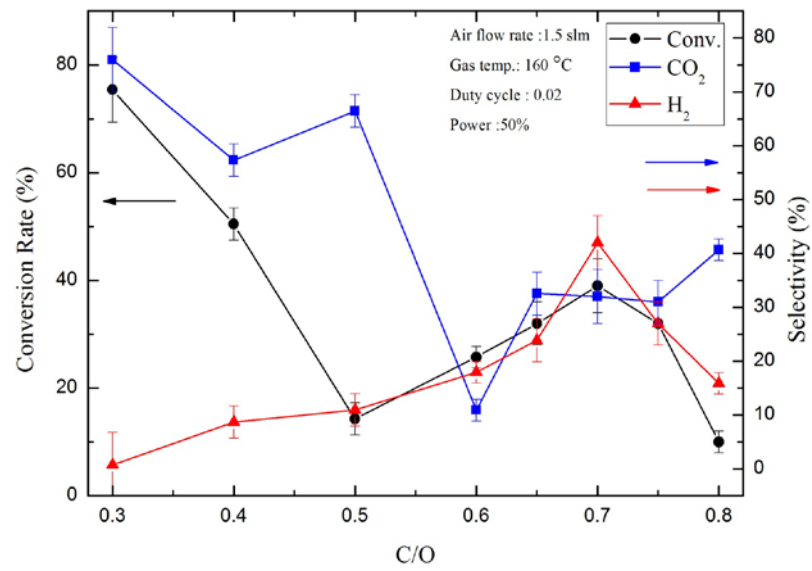
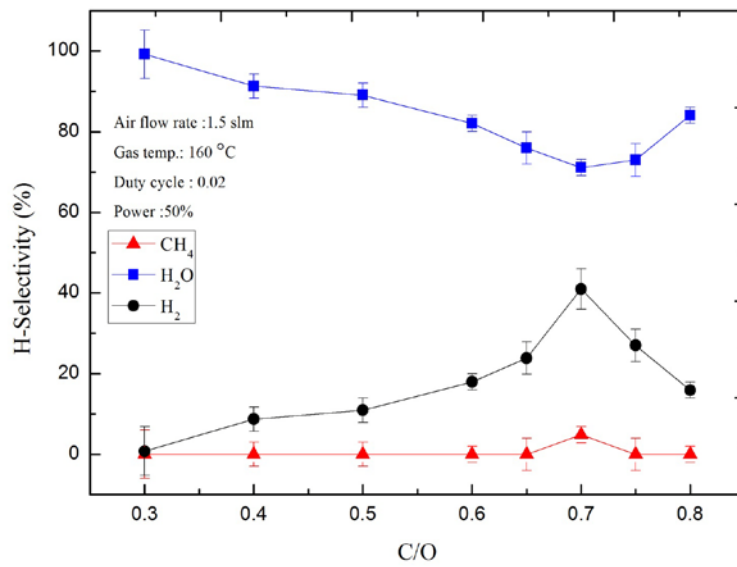Figure 3.17 Conversion rate, S_{H2} and S_{CO2} versus C/O ratio.

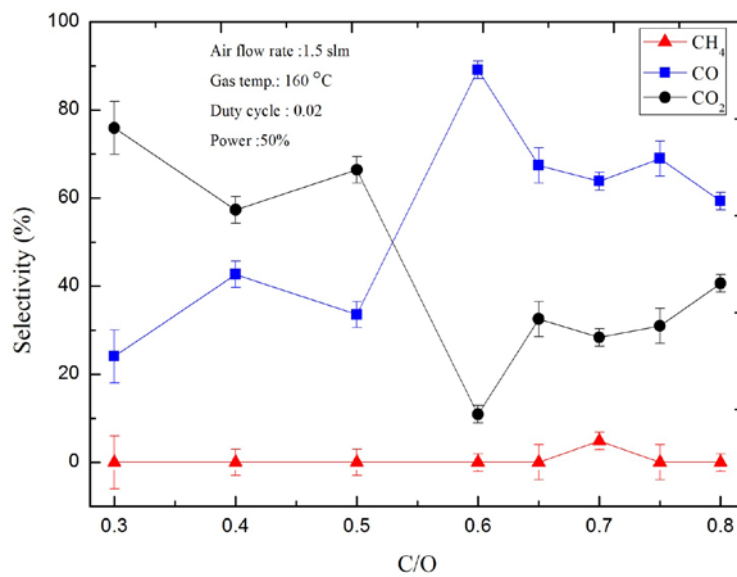Figure 3.18 S_{H2}, S_{H2O} and S_{CH4} versus C/O ratio.
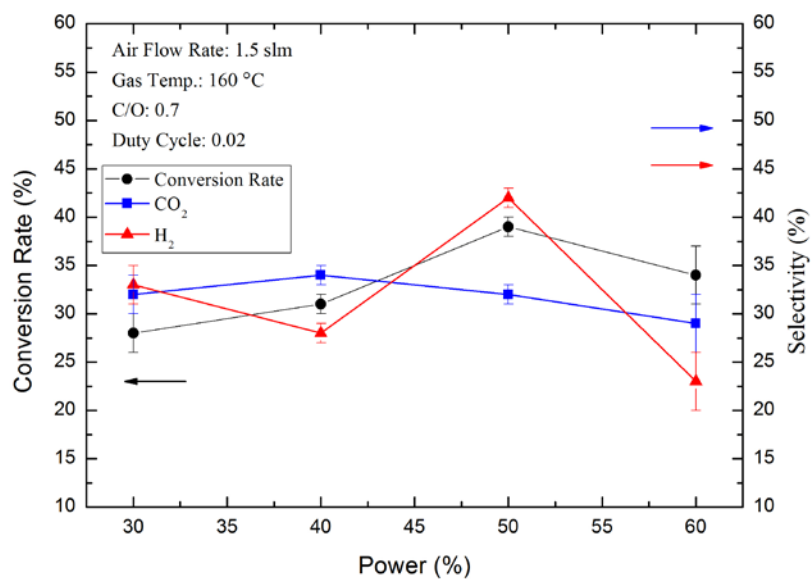

Figure 3.19 SCO2, SCO and SCH4 versus C/O ratio.

Figure 3.20 Conversion rate, S_{H2} and S_{CO2} versus plasma power input.